

# Inflation and dark matter after spontaneous Planck scale generation by hidden chiral symmetry breaking

Mayumi Aoki,<sup>1, a</sup> Jisuke Kubo,<sup>2, 3, b</sup> and Jinbo Yang<sup>1, c</sup>

<sup>1</sup>*Institute for Theoretical Physics, Kanazawa University, Kanazawa 920-1192, Japan*

<sup>2</sup>*Max-Planck-Institut für Kernphysik (MPIK),*

*Saupfercheckweg 1, 69117 Heidelberg, Germany*

<sup>3</sup>*Department of Physics, University of Toyama,*

*3190 Gofuku, Toyama 930-8555, Japan*

Dynamical chiral symmetry breaking in a QCD-like hidden sector is used to generate the Planck mass and the electroweak scale including the heavy right-handed neutrino mass. A real scalar field transmits the energy scale of the hidden sector to the visible sectors, playing besides a role of inflaton in the early Universe while realizing a Higgs-inflation-like model. Our dark matter candidates are hidden pions that raise due to dynamical chiral symmetry breaking. They are produced from the decay of inflaton. Unfortunately, it will be impossible to directly detect them, because they are super heavy ( $10^9 \sim 10^{12}$  GeV), and moreover the interaction with the visible sector is extremely suppressed.

## I. INTRODUCTION

While the standard model (SM) has been successful in explaining a large number of experimental data, the model fails to answer several questions, such as the neutrino mass, dark matter (DM), matter-antimatter asymmetry, and inflation. Neutrino masses cannot be explained with only the field content of the SM; there are no viable candidates for DM; asymmetry of matter and antimatter in our Universe has been addressed for a long time as a serious problem; cosmic inflation provides a compelling explanation for the homogeneity and isotropy of the Universe and for the observed spectrum of density perturbations. However, the inflaton's nature remains unknown.

<sup>a</sup> [mayumi.aoki@staff.kanazawa-u.ac.jp](mailto:mayumi.aoki@staff.kanazawa-u.ac.jp)

<sup>b</sup> [kubo@mpi-hd.mpg.de](mailto:kubo@mpi-hd.mpg.de)

<sup>c</sup> [j\\_yang@hep.s.kanazawa-u.ac.jp](mailto:j_yang@hep.s.kanazawa-u.ac.jp)

Furthermore, the SM suffers from a hierarchy problem. The only dimensionful parameter in the SM, the Higgs mass parameter  $\mu_H$  is sensitive to quantum corrections, if there exist high intermediate scales. The correction  $\delta\mu_H^2$  becomes huge as  $\delta\mu_H^2 \sim \Lambda^2$ , where  $\Lambda$  represents the high intermediate scales. This implies that a sizable fine-tuning between various contributions to the Higgs mass is needed.

Similarly to the SM case, in which  $\mu_H$  is the only dimensionful parameter, Einstein's theory of gravity contains a single dimensionful parameter, the Planck mass (apart from the cosmological constant), and classical scale invariance forbids the presence of these dimensionful parameters in the Lagrangian. Thus our guiding principle to construct a model in this paper is scale invariance. Though scale invariance is anomalous, anomaly can not directly generate mass gaps. Consequently, scale invariance has to be spontaneously broken to generate a mass gap - a physical energy scale. One possible method to generate a scale is the dynamical way by the Coleman-Weinberg potential [1]. Another possibility is the non-perturbative way in nonabelian gauge theories, e.g., Quantum Chromodynamics (QCD) [2–4]. In the present paper we ask ourselves whether it is possible to generate the Planck mass and the electroweak scale from the same origin. In this way a new view on the hierarchy problem may be gained, because the hierarchy problem is a problem among different mass scales.

If one is to maintain classical scale invariance in a complete theory including the gravity, therefore, it is necessary to generate the Planck mass, through the spontaneous breaking of the scale invariance [5–8]. This is realized in, e.g., the Brans-Dicke theory [5] where the  $M_{\text{Pl}}$  is generated dynamically by the vacuum expectation value (VEV) of a scalar field. The non-minimal coupling term  $S^2R$  generates the effective Einstein-Hilbert term, where  $S$  is a real scalar field and  $R$  is the Ricci scalar. This scenario incorporates inflation while identifying the scalar field as inflaton [9–28]. In this case, the Planck mass is dynamically generated during or before inflation.

In this paper, we construct a classical scale invariant model with  $R + R^2$  gravity [29–31] where the Planck mass is generated dynamically by the VEV of an inflaton. The original  $R^2$  inflation is known as the Starobinsky inflation [29], in which inflaton is the degree of freedom related to the  $R^2$  term [32, 33]. Predictions of the  $R^2$  inflation, such as a spectral index  $n_s$  and a tensor-to-scalar ratio  $r$ , fit observations in the Planck experiment [34, 35] very well. In scale invariant extensions of the  $R^2$  inflation model, on the other hand, a double-field

inflation system is realized due to the non-minimal coupling  $S^2R$  [17–21].

We introduce a strongly interacting QCD-like hidden sector, in which the mass scale is generated in a non-perturbative way via condensation that breaks chiral symmetry dynamically. The Higgs mass is generated by the quantum correction. We apply the “Neutrino option” [36], where  $\mu_H^2$  is generated by the quantum correction of the right-handed neutrinos. To obtain a consistent scale in the neutrino option scenario, the masses of the right-handed neutrinos are  $\sim 10^7$  GeV [37–40]. The Majorana mass term of the right-handed neutrino is dynamically generated via the chiral symmetry breaking [41, 42], while the light active neutrinos obtain the masses through the type-I seesaw mechanism [43–46]. In this model, there exist (quasi) Nambu-Goldstone (NG) bosons due to the dynamical chiral symmetry breaking, and due to their stability they are good DM candidates [47–52].

The paper is organized as follows. In Section II, we introduce the scale invariant model with a QCD-like hidden sector. We use Nambu-Jona-Lasinio (NJL) model as an effective low-energy theory in a mean field approximation. The masses of Planck, neutrinos, and Higgs boson are discussed. In Section III, we show an effective action and discuss the inflationary dynamics in our model. The results of the numerical study for the predicted inflation parameters are presented. In Section IV, we discuss the DM candidates which are produced during or after the reheating phase. The reheating temperature and the DM relic abundance are computed. We summarize and conclude in Section V.

## II. THE MODEL

Our model should describe (i) the generation of a robust energy scale through the formation of chiral condensate, (ii) gravity, (iii) the SM interactions, (iv) including heavy right-handed neutrinos. We impose scale invariance, and therefore no part of the model should contain any dimensionful parameter at the classical level.

(i) In this part of the model, a robust energy scale is generated, which is the unified origin of energy scales of other sectors. Instead of the Coleman-Weinberg mechanism [1] which has been used for the unified origin of energy scales in [16], we employ here a strongly-interacting, QCD-like theory in which chiral symmetry is dynamically broken [2–4] and as

a result a robust energy scale is generated. This part is described by

$$\frac{\mathcal{L}_H}{\sqrt{-g}} = -\frac{1}{2}\text{Tr} F^2 + \text{Tr} \bar{\psi}(i\not{D} - \mathbf{y}S)\psi, \quad (2.1)$$

where  $F$  is the matrix-valued field strength tensor of the  $SU(N_c)_H$  gauge theory, coupled with the vector-like hidden fermions  $\psi_i$  ( $i = 1, \dots, n_f$ ) belonging to the fundamental representation of  $SU(n_c)_H$ , and  $S$  is a real SM singlet scalar. The strong dynamics of the QCD-like theory (2.1) forms a gauge invariant chiral condensate  $\langle \bar{\psi}\psi \rangle$ , which generates a linear term in  $S$  in the potential, leading to a nonzero VEV of  $S$  [47–50]. The scalar  $S$  plays a role of the mediator, because it subsequently transfers the robust energy scale to the other sectors of the model.  $\mathbf{y}$  is an  $n_f \times n_f$  Yukawa coupling matrix which can be assumed as a diagonal matrix without loss of generality, i.e.  $\mathbf{y} = \text{diag.}(y_1, \dots, y_{n_f})$ . This Yukawa coupling violates explicitly chiral symmetry. Consequently, the NG bosons, associated with the dynamical chiral symmetry breaking  $SU(n_f)_L \times SU(n_f)_R \rightarrow SU(n_f)_V$ , acquire their masses and can become DM candidates due to the remnant unbroken flavor group  $SU(n_f)_V$  (or its subgroup, depending on the choice of  $y_i$ ) that can stabilise them [47–50]. Note that due to the presence of the fermions the use of the vierbein formalism is quietly understood. But it does not play any role in the following discussions.

(ii) This part is described by the Lagrangian

$$\frac{\mathcal{L}_G}{\sqrt{-g}} = -\frac{\beta}{2} S^2 R + \gamma R^2 + \kappa W_{\mu\nu\alpha\beta} W^{\mu\nu\alpha\beta}, \quad (2.2)$$

where  $R$  denotes the Ricci curvature scalar, and  $W_{\mu\nu\alpha\beta}$  is the Weyl tensor. The Ricci curvature tensor squared,  $R_{\mu\nu\alpha\beta} R^{\mu\nu\alpha\beta}$ , is omitted in the Lagrangian (2.2), because it (and also  $R_{\mu\nu} R^{\mu\nu}$ ) can be written as a linear combination of  $R^2$ ,  $W_{\mu\nu\alpha\beta} W^{\mu\nu\alpha\beta}$  and the Gauß-Bonnet term which is a surface term. The non-minimal coupling  $S^2 R$  produces the Einstein-Hilbert term when the real scalar field  $S$  acquires the VEV denoted by  $v_S$ , with the (reduced) Planck mass  $M_{\text{Pl}} \simeq \sqrt{\beta} v_S$ . Then the scalar  $S$  and the scalaron  $\varphi$  [29], which describes the scalar degree of freedom related to the  $R^2$  term, form a double-filed inflaton system to describe cosmic inflation [17–21].

(iii) The Lagrangian of this part consists of the SM Lagrangian with the Higgs mass term suppressed,  $\mathcal{L}_{\text{SM}}|_{\mu_H=0}$ , and also of the Lagrangian for  $S$ :

$$\frac{\mathcal{L}_{\text{SM}+S}}{\sqrt{-g}} = \frac{\mathcal{L}_{\text{SM}}|_{\mu_H=0}}{\sqrt{-g}} + \frac{1}{2} g^{\mu\nu} \partial_\mu S \partial_\nu S - \frac{1}{4} \lambda_{HS} S^2 H^\dagger H - \frac{1}{4} \lambda_S S^4, \quad (2.3)$$

where  $H$  is the SM Higgs doublet, and  $\mu_H$  is the mass parameter for the Higgs mass term  $\mu_H^2 H^\dagger H$ . As we explain at (iv), the Higgs portal coupling  $\lambda_{HS}$  has to be extremely small, and we will ignore it throughout the following discussions. So, it is just introduced to ensure renormalizability. <sup>1</sup>

(iv) This part of the model is responsible for making the right- and left-handed neutrinos,  $N_R$  and  $\nu_L$ , massive and also for generating the Higgs mass term radiatively:

$$\frac{\mathcal{L}_N}{\sqrt{-g}} = \frac{i}{2} \bar{N}_R \not{\partial} N_R - \frac{1}{2} y_M S N_R^T C N_R - \left( y_\nu \bar{L} \tilde{H} \frac{1 + \gamma_5}{2} N_R + \text{h.c.} \right), \quad (2.4)$$

where  $\tilde{H} = i\sigma_2 H^*$ ,  $L$  is the lepton doublet, and  $C$  is the charge conjugation matrix. Strictly speaking, the Yukawa couplings  $y_\nu$  and  $y_M$  should be matrices in the generation space. However, we will not consider the flavor structure, instead  $y_\nu$  and  $y_M$  will be representative real numbers. The right-handed neutrinos  $N_R$  become massive due to the second term on the rhs of Eq. (2.4) when  $S$  acquires the VEV, i.e.  $m_N = y_M v_S$ . We assume that  $m_N \sim 10^7$  GeV to obtain a desired size of the radiative correction to  $\mu_H^2$  [37–40] for triggering the electroweak symmetry breaking and at the same to make the type-I seesaw mechanism [43–46] viable - a scenario dubbed the “Neutrino option” [16, 36, 42, 53–58]. In this scenario it is assumed that the radiative correction is the dominant contribution to  $\mu_H^2$  while the tree-level contribution  $\lambda_{HS} v_S^2/4$  is negligibly small [42, 54].

As we have seen above, the real scalar field  $S$  appears in all the sectors. It is the mediator that transfers the robust energy scale, created by the chiral condensate, to the gravity sector, while playing a role of inflaton on one hand, and is on the other hand responsible for generating the heavy right-handed neutrinos, which in turn give rise to the electroweak symmetry breaking as well as to the light active neutrinos.

### A. Origin of the unified energy scale:

#### Nambu-Jona-Lasinio description of chiral symmetry breaking

Lattice gauge theory is a first-principle calculation in the QCD-like hidden sector that is described by the Lagrangian (2.1). Here we shall use an effective field theory - the NJL

<sup>1</sup> We assume that the  $H^\dagger H R$  coupling is negligibly small, such that the Higgs plays no role in our scenario of inflation.

theory [2–4] - to describe the dynamical chiral symmetry breaking in the hidden sector.<sup>2</sup> Following Refs. [49, 51, 52] we assume  $n_f = n_c = 3$ , because in this case the meson properties in hadron physics can be used to reduce the independent parameters of the NJL theory [49, 51, 52]. So, the hidden chiral symmetry is  $SU(3)_L \times SU(3)_R$ , which is dynamically broken to its diagonal subgroup  $SU(3)_V$  by the non-zero chiral condensate  $\langle \bar{\psi}\psi \rangle$ , implying the existence of 8 NG bosons.

The NJL Lagrangian for the hidden sector<sup>3</sup> is given by [2–4]

$$\mathcal{L}_{\text{NJL}} = \text{Tr} \bar{\psi}(i\cancel{\partial} - \mathbf{y}S)\psi + 2G \text{Tr} \Phi^\dagger \Phi + G_D (\det \Phi + h.c.), \quad (2.5)$$

where

$$\Phi_{ij} = \bar{\psi}_i(1 - \gamma_5)\psi_j = \frac{1}{2} \sum_{a=0}^8 \lambda_{ji}^a [\bar{\psi}\lambda^a(1 - \gamma_5)\psi], \quad (2.6)$$

$\lambda^a (a = 1, \dots, 8)$  are the Gell-Mann matrices with  $\lambda^0 = \sqrt{2/3} \mathbf{1}$ , and the canonical dimension of  $G$  ( $G_D$ ) is  $-2$  (5). Further, we use the self-consistent mean-field (SCMF) approximation of Refs. [59, 60] and define the mean fields  $\sigma_i$  ( $i = 1, 2, 3$ ) and  $\phi_a$  ( $a = 0, \dots, 8$ ) in the ‘‘Bardeen-Cooper-Schrieffer’’ vacuum as

$$\sigma_i = -4G \langle \bar{\psi}_i \psi_i \rangle, \quad \phi_a = -2iG \langle \bar{\psi}_i \gamma_5 \lambda^a \psi_i \rangle, \quad (2.7)$$

respectively. Here we suppress the CP-even mean fields corresponding to the non-diagonal elements of  $\langle \bar{\psi}_i \psi_j \rangle$ , because they do not play any role for our purpose.<sup>4</sup> Then splitting the NJL Lagrangian  $\mathcal{L}_{\text{NJL}}$  into two parts as  $\mathcal{L}_{\text{NJL}} = \mathcal{L}_{\text{MFA}} + \mathcal{L}_I$  where  $\mathcal{L}_I$  is normal ordered (i.e.,  $\langle 0|\mathcal{L}_I|0\rangle = 0$ ), we find the mean-field Lagrangian  $\mathcal{L}_{\text{MFA}}$  in the SCMF approximation:<sup>5</sup>

$$\begin{aligned} \mathcal{L}_{\text{MFA}} = & \text{Tr} \bar{\psi}(i\cancel{\partial} - M)\psi - i\text{Tr} \bar{\psi}\gamma_5\phi\psi - \frac{1}{8G} \left( 3\sigma^2 + 2 \sum_{a=1}^8 \phi_a \phi_a \right) \\ & + \frac{G_D}{8G^2} \left( -\text{Tr} \bar{\psi}\phi^2\psi + \sum_{a=1}^8 \phi_a \phi_a \text{Tr} \bar{\psi}\psi + i\sigma \text{Tr} \bar{\psi}\gamma_5\phi\psi + \frac{\sigma^3}{2G} + \frac{\sigma}{2G} \sum_{a=1}^8 (\phi_a)^2 \right), \end{aligned} \quad (2.8)$$

<sup>2</sup> Linear sigma model is used in Ref. [47], and the holographic method is applied in Ref. [50].

<sup>3</sup> Here we work in the flat space time.

<sup>4</sup> The lightest of  $\sigma_i$  behaves as the dilaton [59, 60], the (quasi) NG boson associated with the spontaneous breaking of scale invariance. It is massive, because scale invariance is explicitly broken by anomaly at the fundamental level and by four and six Fermi interactions (2.5) at the effective level.

<sup>5</sup> The mean-field Lagrangian  $\mathcal{L}_{\text{MFA}}$  in the case of broken  $SU(3)_V$  can be found in Ref. [52].

where  $\phi = \sum_{a=1}^8 \phi_a \lambda^a$ ,  $\sigma = \sigma_1 = \sigma_2 = \sigma_3$ , and  $\phi_0$  has been suppressed. The constituent fermion mass  $M$  is given by

$$M(S, \sigma) = \sigma + yS - \frac{G_D}{8G^2} \sigma^2, \text{ where } y = y_1 = y_2 = y_3. \quad (2.9)$$

The one-loop effective potential can be obtained from  $\mathcal{L}_{\text{MFA}}$  (2.8) by integrating out the hidden fermions:

$$V_{\text{NJL}}(S, \sigma) = \frac{3}{8G} \sigma^2 - \frac{G_D}{16G^3} \sigma^3 - 3n_c I_0(M, \Lambda_H), \quad (2.10)$$

where the function  $I_0$  is given by

$$I_0(M, \Lambda) = \frac{1}{16\pi^2} \left[ \Lambda^4 \ln \left( 1 + \frac{M^2}{\Lambda^2} \right) - M^4 \ln \left( 1 + \frac{\Lambda^2}{M^2} \right) + \Lambda^2 M^2 \right], \quad (2.11)$$

with a four-dimensional momentum cutoff  $\Lambda$ .<sup>6</sup> Note that the cutoff parameter  $\Lambda$  is an additional free parameter in the NJL theory. For a certain interval of the dimensionless parameters,  $G^{1/2}\Lambda$  and  $(-G_D)^{1/5}\Lambda$ , we have  $v_\sigma = \langle \sigma \rangle \neq 0$  and  $v_S = \langle S \rangle \neq 0$  [49, 51, 52]. The actual value of  $\Lambda$  can be fixed, once the hidden sector is connected with a sector whose energy scale is given. In our case, the hidden sector is coupled via the mediator  $S$  with the gravity sector (ii) described by Eq. (2.2) as well as with the right-handed neutrino sector (iv) described by Eq. (2.4), while the coupling with the SM sector (iii) is assumed to be extremely suppressed, because we assume that the portal coupling  $\lambda_{HS}$  is negligibly small. Hereafter we will denote the cutoff in our hidden sector by  $\Lambda_H$ . It can be fixed in the following way.

The NJL parameters for the SM hadrons satisfy the dimensionless relations [49, 51, 52]  $G^{1/2}\Lambda|_{\text{Hadron}} = 1.82$  and  $(-G_D)^{1/5}\Lambda|_{\text{Hadron}} = 2.29$ , where  $\Lambda_{\text{Hadron}} \simeq 0.1$  GeV. We assume that the above dimensionless relations are satisfied while scaling-up the values of  $G, G_D$  and the cutoff  $\Lambda$  from QCD hadron physics:

$$G^{1/2}\Lambda|_{\text{Hidden}} = 1.82, \quad (-G_D)^{1/5}\Lambda|_{\text{Hidden}} = 2.29, \quad (2.12)$$

should remain unchanged for  $\Lambda_{\text{Hidden}} = \Lambda_H \gg \Lambda_{\text{Hadron}}$ .

It is noted that the mean fields  $\sigma$  and  $\phi_a$  are non-propagating classical fields at the tree level. Therefore, their kinetic terms are generated by integrating out the hidden fermions

---

<sup>6</sup> The one-loop correction  $I_0(M, \Lambda)$  in a curved space time has been calculated in Ref. [61, 62]. It is proportional to  $(\sigma^2/96\pi^2)R$ , which is a minimal coupling like  $\beta S^2 R$ . However, since  $\beta = O(1) - O(10^4)$  as we will see when discussing inflation, this additional term in the curved space time is negligible compared to the tree-level term  $\beta S^2 R$ .

at the one-loop level, which will be seen in Section IV A, where two point functions are calculated. Further, one can see that the potential  $V_{\text{NJL}}(S, \sigma)$  is asymmetric in  $\sigma$  by inspecting the last term in the NJL Lagrangian in Eq. (2.8) as well as the constituent mass  $M$  in Eq. (2.9); due to latter chiral phase transition can become of first-order [63–65].

## B. Planck mass

We next integrate out the quantum fluctuations  $\delta S$  at one-loop to obtain the effective potential

$$U_S(S, R) = \frac{1}{4}\lambda_S S^4 + \frac{1}{64\pi^2} (\tilde{m}_s^4 \ln[\tilde{m}_s^2/\mu^2]) , \quad (2.13)$$

where

$$\tilde{m}_s^2 = 3\lambda_S S^2 + \beta R . \quad (2.14)$$

Here we have used the  $\overline{\text{MS}}$  scheme, and the constant  $-3/2$  is absorbed into the renormalization scale  $\mu$ .<sup>7</sup> Our total effective potential in the Jordan frame now reads

$$U_{\text{eff}}(S, \sigma, R) = V_{\text{NJL}}(S, \sigma) + U_S(S, R) - U_0 , \quad (2.15)$$

where  $V_{\text{NJL}}$  is given in Eq. (2.10), and  $U_0$  is the zero-point energy density. We have subtracted it, such that  $U_{\text{eff}}(S = v_S, \sigma = v_\sigma, R = 0) = 0$  is satisfied. The zero-point energy density  $U_0$  is negative, because it is a consequence of the spontaneous breaking of global conformal symmetry. Subtracting  $U_0$  means that we start with a nonzero cosmological constant. That is, we add an explicit super-soft breaking of scale invariance at tree level, and accordingly we put the cosmological constant problem [67] aside here and continue with our discussion.

To compute  $v_S = \langle S \rangle$  and  $v_\sigma = \langle \sigma \rangle$ , we assume that  $\beta R < 3\lambda_S S^2$  (during inflation), such that  $U_S(S, R)$  in Eq. (2.13) can be expanded in powers of  $\beta R$ :

$$U_S(S, R) = U_{\text{CW}}(S) + U_{(1)}(S) R + U_{(2)}(S) R^2 + O(R^3) , \quad (2.16)$$

where

$$U_{\text{CW}}(S) = \frac{1}{4}\lambda_S S^4 + \frac{9}{64\pi^2} \lambda_S^2 S^4 \left( \ln[3\lambda_S S^2/v_S^2] - \frac{1}{2} \right) , \quad (2.17)$$

---

<sup>7</sup> Strictly speaking,  $\beta$  in Eq. (2.14) should read  $\beta - 1/6$ , if one properly takes into account the non-flatness of space-time background and the integration of the quantum fluctuations [66]. However, since  $\beta$  will turn out be large (i.e.  $\gtrsim 4$ ) for realistic cosmic inflation, we will be ignoring the constants  $1/6$  throughout the paper.



$$U_{(1)}(S) = \frac{3}{32\pi^2} \beta \lambda_S S^2 \ln[3\lambda_S S^2/v_S^2], \quad (2.18)$$

$$U_{(2)}(S) = \frac{1}{64\pi^2} \beta^2 (1 + \ln[3\lambda_S S^2/v_S^2]). \quad (2.19)$$

We have chosen  $\mu^2 = v_S^2/2$ , such that we can calculate  $v_S$  from  $V_{\text{NJL}}(S, \sigma) + \lambda_S S^4/4$  (i.e. the logarithmic term does not enter into the determination of  $v_S$  and  $v_\sigma$ ). Since we are assuming a negligibly small (but, of course, nonzero during inflation) value of the curvature scalar  $R$ , we obtain the  $R$ -independent leading-order  $v_S$  and  $v_\sigma$  from  $V_{\text{NJL}}(S, \sigma) + \lambda_S S^4/4$ . Finally, the identification of  $M_{\text{Pl}}$  follows from the first term in Eq. (2.2) along with Eq. (2.16):

$$M_{\text{Pl}} = v_S \left( \beta + \frac{2U_{(1)}(v_S)}{v_S^2} \right)^{1/2} = \sqrt{\beta} v_S \left( 1 + \frac{3\lambda_S}{16\pi^2} \ln[3\lambda_S] \right)^{1/2}. \quad (2.20)$$

As we will see,  $\beta$  is of order  $10^3$  for a successful inflation,  $v_S$  is few orders of magnitude smaller than  $M_{\text{Pl}}$ .

### C. Neutrino mass and Higgs mass

The basic idea of the neutrino option is already explained in Section II. Here we briefly discuss how the mass hierarchy is realized in our model. Since for the neutrino option to work, we require  $m_N = y_M v_S \sim 10^7$  GeV, where  $y_M$  is the Majorana-Yukawa coupling in the sector (iv) described by the Lagrangian (2.4). On the other hand, we have  $v_S \simeq M_{\text{Pl}}/\sqrt{\beta}$  from Eq. (2.20), which implies  $y_M \sim \sqrt{\beta} 10^{-11}$ . Therefore, the Majorana-Yukawa coupling  $y_M$  has to be very small. Note however that the small  $y_M$  is not unnatural, because in its absence the lepton number is conserved. Compared with  $m_H/M_{\text{Pl}} \sim 10^{-16}$ , where  $m_H \simeq 125$  GeV is the SM Higgs mass, this original mass hierarchy  $10^{-16}$  can be largely softened for  $\beta$  large. Note also that  $m_H^2 \sim y_\nu^2 m_N^2/4\pi^2$  in the neutrino option, where  $y_\nu$  is the Dirac-Yukawa coupling. This equation implies  $m_H^4 \sim \lambda_H m_\nu m_N^3/4\pi^2$ , where  $\lambda_H$  is the Higgs quartic coupling in Eq. (2.3) and  $m_\nu$  stands for the light neutrino mass. That is, the scale of the Higgs mass is basically fixed by the neutrino sector, which is a consequence of the fact that the SM is only indirectly coupled with the hidden sector through a negligibly small portal coupling  $\lambda_{HS}$ .

### III. INFLATION

#### A. Effective action for inflation

If the inequality  $\beta R < 3\lambda_S S^2$  is satisfied during inflation, the higher order terms in Eq. (2.16) can be consistently neglected for inflation. We will proceed with this simplification, but we will posteriori check whether the inequality is satisfied. Similarly, if  $\kappa$ , the coefficient of the  $W_{\mu\nu\alpha\beta}W^{\mu\nu\alpha\beta}$  term in Eq. (2.2), is small, this term has only a small effect on the inflationary parameters (see for instance [25]), so that we will ignore it in the following discussion as well.<sup>8</sup> In doing so, we arrive at the effective Lagrangian for inflation in the Jordan frame

$$\frac{\mathcal{L}_{\text{eff}}}{\sqrt{-g_J}} = -\frac{1}{2}M_{\text{Pl}}^2 B(S)R_J + G(S)R_J^2 + \frac{1}{2}g_J^{\mu\nu} (\partial_\mu S \partial_\nu S + Z_\sigma^{-1}(S, \sigma) \partial_\mu \sigma \partial_\nu \sigma) - U(S, \sigma), \quad (3.1)$$

where

$$B(S) = \frac{\beta S^2}{M_{\text{Pl}}^2} \left( 1 + \frac{3\lambda_S}{16\pi^2} \ln[3\lambda_S S^2/v_S^2] \right), \quad (3.2)$$

$$G(S) = \gamma - \frac{\beta^2}{64\pi^2} (1 + \ln[3\lambda_S S^2/v_S^2]), \quad (3.3)$$

$$U(S, \sigma) = V_{\text{NJL}}(S, \sigma) + \frac{\lambda_S}{4} S^4 + \frac{9\lambda_S^2 S^4}{64\pi^2} \left( -\frac{1}{2} + \ln[3\lambda_S S^2/v_S^2] \right) - U_0. \quad (3.4)$$

Here  $g_J^{\mu\nu}$  ( $g_J = \det g_{\mu\nu}^J$ ) and  $R_J$  denote the inverse of the metric  $g_{\mu\nu}^J$  and the Ricci scalar of Jordan-frame space time, respectively. To remove the  $R_J^2$  term from Eq. (3.1), we introduce an auxiliary field  $\chi$  with mass dimension two and replace  $G(S)R_J^2$  by  $2G(S)R_J\chi - G(S)\chi^2$ . Then performing a Weyl rescaling of the metric,  $g_{\mu\nu} = \Omega^2 g_{\mu\nu}^J$  with

$$\Omega^2(S, \chi) = B(S) - \frac{4G(S)\chi}{M_{\text{Pl}}^2}, \quad (3.5)$$

we arrive at the Einstein frame with the Lagrangian

$$\frac{\mathcal{L}_{\text{eff}}^E}{\sqrt{-g}} = -\frac{1}{2}M_{\text{Pl}}^2 \left( R - \frac{3}{2}g^{\mu\nu} \partial_\mu \ln \Omega^2(S, \chi) \partial_\nu \ln \Omega^2(S, \chi) \right)$$

<sup>8</sup> The presence of the  $W_{\alpha\beta\mu\nu}W^{\alpha\beta\mu\nu}$  in (22) causes theoretical problems: The classical Hamiltonian is bounded from below (Ostrogradsky instability). Furthermore, the massive (after the spontaneous scale symmetry breaking) spin two state is a ghost state [68], due to the wrong sign of its kinetic term (see also [69]). Therefore, this state endangers unitarity of the theory. Although no ultimate solution seems to exist to this problem at present, there are various interesting Ansätze, which is reviewed for instance in [70]. We do not address this problem here, because this would be beyond the scope of the present paper.

$$+ \frac{g^{\mu\nu}}{2\Omega^2(S, \chi)} (\partial_\mu S \partial_\nu S + Z_\sigma^{-1}(S, \sigma) \partial_\mu \sigma \partial_\nu \sigma) - V(S, \sigma, \chi), \quad (3.6)$$

where

$$V(S, \sigma, \chi) = \frac{U(S, \sigma) + G(S)\chi^2}{[B(S)M_{\text{Pl}}^2 - 4G(S)\chi]^2} M_{\text{Pl}}^4. \quad (3.7)$$

Note that  $\chi$  is promoted to a propagating scalar field in the Einstein frame. Using the scalaron field  $\varphi$  [32, 33], which is canonically normalized and defined as

$$\varphi = \sqrt{\frac{3}{2}} M_{\text{Pl}} \ln |\Omega^2|, \quad (3.8)$$

we finally obtain the Einstein-frame Lagrangian for the coupled  $S$ - $\sigma$ -scalaron system:

$$\begin{aligned} \frac{\mathcal{L}_{\text{eff}}^E}{\sqrt{-g}} = & -\frac{1}{2} M_{\text{Pl}}^2 R + \frac{1}{2} g^{\mu\nu} \partial_\mu \varphi \partial_\nu \varphi + \frac{1}{2} e^{-\Phi(\varphi)} g^{\mu\nu} (\partial_\mu S \partial_\nu S + Z_\sigma^{-1}(S, \sigma) \partial_\mu \sigma \partial_\nu \sigma) \\ & - V(S, \sigma, \varphi), \end{aligned} \quad (3.9)$$

where  $\Phi(\varphi) = \sqrt{2/3} \varphi / M_{\text{Pl}}$ , and the potential  $V$  given in Eq. (3.7) is

$$V(S, \sigma, \varphi) = e^{-2\Phi(\varphi)} \left[ U(S, \sigma) + \frac{M_{\text{Pl}}^4}{16G(S)} (B(S) - e^{\Phi(\varphi)})^2 \right]. \quad (3.10)$$

## B. Valley approximation

As we see from the Lagrangian (3.9) we have a multi-field system at hand [71]. Fortunately, it turns out that the valley approximation [23] can be successfully applied, so that we only have to deal with a single-field inflaton system, as we will see below. To begin with we find that the stationary point condition

$$\left. \frac{\partial V(S, \sigma, \varphi)}{\partial \varphi} \right|_{\varphi=\varphi_v} = 0 \quad (3.11)$$

can be solved analytically for  $\varphi$ :

$$\varphi_v = \sqrt{3/2} M_{\text{Pl}} \ln [B(S) + 4A(S, \sigma)B(S)], \quad \text{where } A(S, \sigma) = \frac{4G(S)U(S, \sigma)}{B^2(S)M_{\text{Pl}}^4}. \quad (3.12)$$

Therefore, the three-field system potential  $V(S, \sigma, \varphi)$  can be reduced to a double-field system potential  $\tilde{V}(S, \sigma) = V(S, \sigma, \varphi_v)$ , which takes the following form:

$$\tilde{V}(S, \sigma) = \frac{U(S, \sigma) M_{\text{Pl}}^4}{16G(S)U(S, \sigma) + B^2(S)M_{\text{Pl}}^4}. \quad (3.13)$$

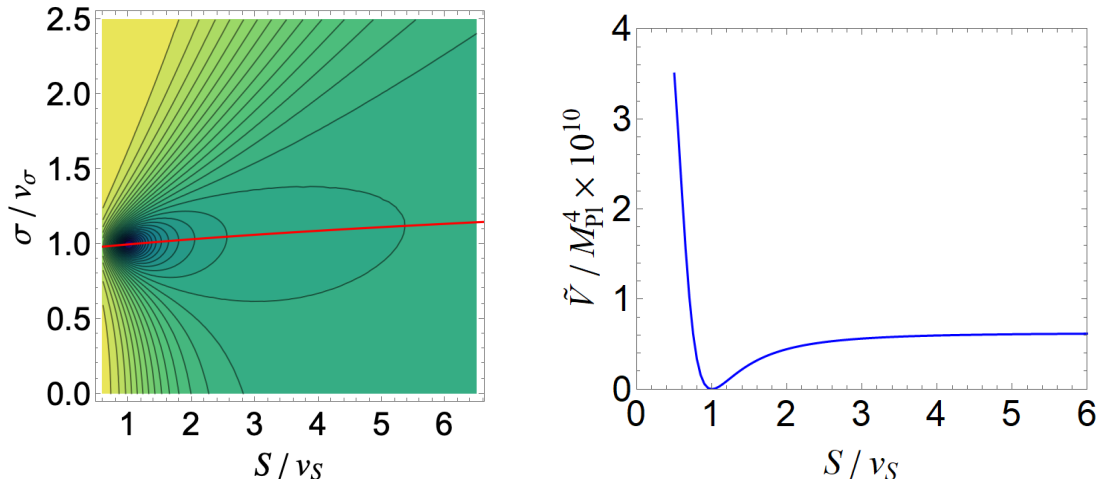


FIG. 1. Left: The contour plot of  $\tilde{V}(S, \sigma)$ , where  $\tilde{V}(S, \sigma) = V(S, \sigma, \varphi_v)$ . The red line is the bottom line of the valley  $\tilde{V}(S, \sigma)$ . Right:  $\tilde{V}(S, \sigma)/M_{\text{Pl}}^4$  along the bottom line of the valley (the red line of the left panel) against  $S/v_S$ .

In Fig. 1 (left) we show a contour plot of  $\tilde{V}(S, \sigma)$  for

$$y = 4.00 \times 10^{-3}, \quad \lambda_S = 1.14 \times 10^{-2}, \quad \beta = 6.31 \times 10^3, \quad \gamma = 1.26 \times 10^8. \quad (3.14)$$

The red line in Fig. 1 (left) is the bottom line of the valley, and we will assume that the inflaton slowly rolls down along this line.  $\tilde{V}(S, \sigma)/M_{\text{Pl}}^4$  along the bottom line of the valley against  $S/v_S$  is plotted in Fig. 1 (right), from which we see that the potential  $\tilde{V}(S, \sigma)$  for  $S/v_S > 1$  along this line is very flat. In Fig. 2 we plot  $m_S^2/m_\sigma^2$  against  $S/v_S$  along the bottom line, where  $m_S^2 = \partial^2 \tilde{V}(S, \sigma)/\partial S^2$  and  $m_\sigma^2 = \partial^2 \tilde{V}(S, \sigma)/\partial \sigma^2$ . We see from Fig. 2 that the second derivative of  $\tilde{V}(S, \sigma)$  with respect to  $\sigma$  is much larger than that with respect to  $S$  along the bottom line, meaning that the perpendicular direction to the bottom line of the valley is much steeper than the parallel direction. This justifies the assumption above that the inflaton slowly rolls down along the bottom line of the valley.

We next consider the potential  $V(S, \sigma_v(S), \varphi)$  given in Eq. (3.10), where  $\sigma_v(S)$  is the bottom line of  $\tilde{V}(S, \sigma)$ . Its contour plot is shown in Fig. 3 (left) for the same set of the parameters as given in Eq. (3.14). We see from the left panel that the potential  $V(S, \sigma_v(S), \varphi)$  has a desired valley structure. We also see from the right panel that the potential  $V(S, \sigma_v(S), \varphi)$  for  $S/v_S > 1$  along the bottom line (the green line of the left panel) is very flat.

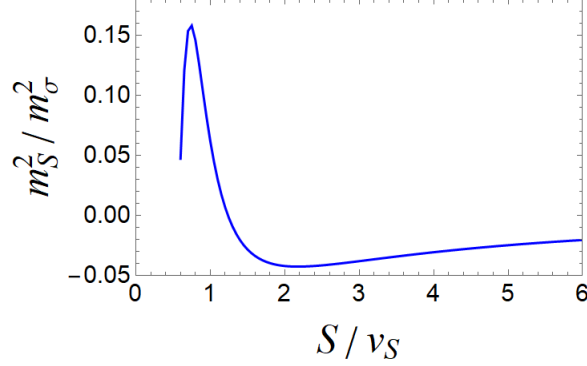


FIG. 2.  $m_S^2/m_\sigma^2$  against  $S/v_S$  along the bottom line of the valley. The graph shows that the perpendicular direction to the bottom line of the valley is much steeper than the parallel direction, so that the inflaton can roll down slowly along the bottom line of the valley.

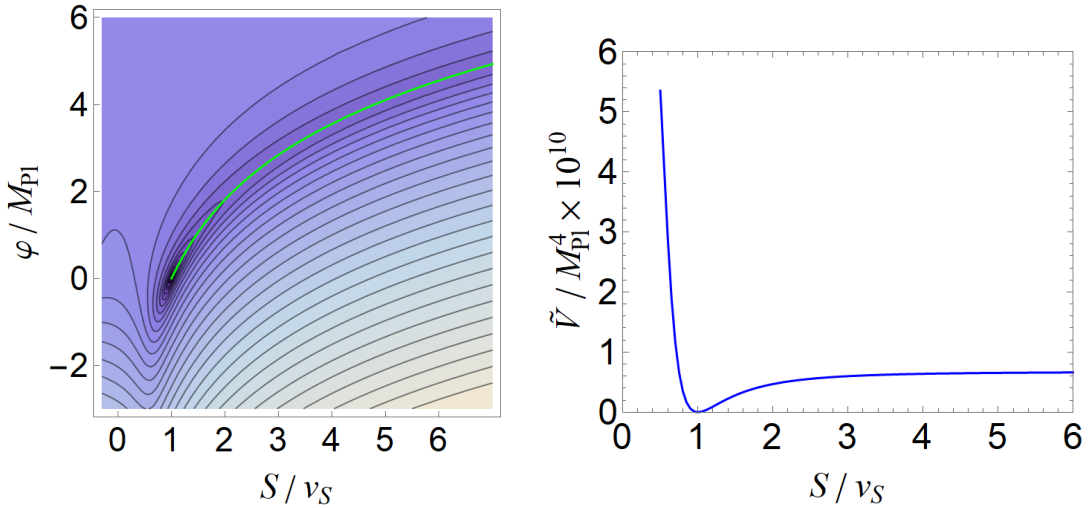


FIG. 3. Left: The contour plot of  $V(S, \sigma_v(S), \varphi)$ , where  $\sigma_v(S)$  is the bottom line of  $\tilde{V}(S, \sigma)$  (the red line of Fig. (1), where of  $V(S, \sigma, \varphi)$  is given in Eq. (3.10). The green line is the bottom line of  $V(S, \sigma_v(S), \varphi)$ , along which the inflaton slowly rolls down. Right:  $V(S, \sigma_v(S), \varphi)/M_{\text{Pl}}^4$  against  $S/v_S$  along the bottom line of  $V(S, \sigma_v(S), \varphi)$  (the blue line of the left panel).

### C. Prediction of the inflationary parameters

The effective Lagrangian for the single-field inflaton system can be obtained from the Lagrangian (3.9), where we treat  $S$  as the independent field variable for the single-field inflaton system. Since  $\sigma$  and  $\varphi$  in this case are functions of  $S$ , their kinetic terms become a

part of the kinetic term for  $S$ :

$$\begin{aligned} & e^{-\Phi(\varphi_v(S))} g^{\mu\nu} \left[ \partial_\mu S \partial_\nu S + Z_\sigma^{-1}(S, \sigma_v) \partial_\mu \sigma_v(S) \partial_\nu \sigma_v(S) \right] + g^{\mu\nu} \partial_\mu \varphi_v(S) \partial_\nu \varphi_v(S) \\ & = F(S)^2 g^{\mu\nu} \partial_\mu S \partial_\nu S, \end{aligned} \quad (3.15)$$

where

$$\begin{aligned} F(S) &= \frac{1}{[1 + 4 A(S, \sigma_v(S))] B(S)} \left\{ [1 + Z_\sigma^{-1}(S, \sigma_v(S)) (\sigma'_v(S))^2] [1 + 4 A(S, \sigma_v(S))] B(S) \right. \\ & \left. + \frac{3}{2} M_{\text{Pl}}^2 \{ [1 + 4 A(S, \sigma_v(S))] B'(S) + 4 A'(S, \sigma_v(S)) B(S) \}^2 \right\}^{1/2}, \end{aligned} \quad (3.16)$$

with  $A(S, \sigma)$  and  $B(S)$  given in Eqs. (3.12) and (3.2), respectively, and the prime stands for derivative with respect to  $S$ . We finally arrive at the single-field inflaton system, which is described by

$$\frac{\mathcal{L}_{\text{eff}}^E}{\sqrt{-g}} = -\frac{1}{2} M_{\text{Pl}}^2 R + \frac{1}{2} F(S)^2 g^{\mu\nu} \partial_\mu S \partial_\nu S - V_{\text{inf}}(S), \quad (3.17)$$

with

$$V_{\text{inf}}(S) = V(S, \sigma_v(S), \varphi_v(S)), \quad (3.18)$$

where  $V(S, \sigma, \varphi)$  and  $\varphi_v$  are given in Eqs. (3.10) and (3.12), respectively, and  $\sigma_v$  is the bottom line of  $\tilde{V}(S, \sigma) = V(S, \sigma, \varphi_v)$ . Note that the canonically normalized inflaton field  $\hat{S}$  can be obtained from

$$\hat{S}(S) = \int_{v_S}^S dx F(x). \quad (3.19)$$

However, to compute the slow roll parameters we will use  $S$  instead of  $\hat{S}$ :

$$\varepsilon(S) = \frac{M_{\text{Pl}}^2}{2 F^2(S)} \left( \frac{V'_{\text{inf}}(S)}{V_{\text{inf}}(S)} \right)^2, \quad (3.20)$$

$$\eta(S) = \frac{M_{\text{Pl}}^2}{F^2(S)} \left( \frac{V''_{\text{inf}}(S)}{V_{\text{inf}}(S)} - \frac{F'(S)}{F(S)} \frac{V'_{\text{inf}}(S)}{V_{\text{inf}}(S)} \right). \quad (3.21)$$

The number of e-folds  $N_e$  can be computed from

$$N_e = \int_{S_{\text{end}}}^{S_*} dS \frac{F^2(S) V_{\text{inf}}(S)}{M_{\text{Pl}}^2 V'_{\text{inf}}(S)}, \quad (3.22)$$

where  $S_*$  is the value of  $S$  at the time of CMB horizon exit, and  $S_{\text{end}}$  is that of  $S$  at the end of inflation, i.e.  $\varepsilon(S = S_{\text{end}}) = 1$ . The CMB observables - the scalar power spectrum

amplitude  $A_s$ , the scalar spectral index  $n_s$  and the tensor-to-scalar ratio  $r$  - can be obtained from

$$A_s = \frac{V_{\text{inf}*}}{24\pi^2 \varepsilon_* M_{\text{Pl}}^4}, \quad n_s = 1 + 2\eta_* - 6\varepsilon_*, \quad r = 16\varepsilon_*, \quad (3.23)$$

where the quantities with  $*$  are evaluated at  $S = S_*$ . In the following discussions we constrain the parameter space spanned by  $y, \lambda_S, \beta$  and  $\gamma$ , such that

$$\ln(10^{10} A_s) = 3.044 \pm 0.014 \text{ and } 50 \lesssim N_e \lesssim 60 \quad (3.24)$$

are satisfied [34, 35].

For the set of the parameters (3.14) we obtain

$$n_s = 0.964, \quad r = 2.00 \times 10^{-3}, \quad \ln(10^{10} A_s) = 3.04, \quad N_e = 55.5, \quad (3.25)$$

where

$$\begin{aligned} v_\sigma/M_{\text{Pl}} &= 8.86 \times 10^{-3}, \quad v_S/M_{\text{Pl}} = 1.26 \times 10^{-2}, \quad U_0/M_{\text{Pl}}^4 = -7.02 \times 10^{-10}, \\ S_{\text{end}}/v_S &= 1.40, \quad S_*/v_S = 6.25, \quad \Lambda_H/M_{\text{Pl}} = 5.33 \times 10^{-2}, \end{aligned} \quad (3.26)$$

and for

$$y = 4.00 \times 10^{-4}, \quad \lambda_S = 1.2 \times 10^{-2}, \quad \beta = 1.435 \times 10^3, \quad \gamma = 5.293 \times 10^8, \quad (3.27)$$

we obtain

$$\begin{aligned} n_s &= 0.963, \quad r = 3.44 \times 10^{-3}, \quad \ln(10^{10} A_s) = 3.04, \quad N_e = 55.0, \\ v_\sigma/M_{\text{Pl}} &= 3.97 \times 10^{-2}, \quad v_S/M_{\text{Pl}} = 2.64 \times 10^{-2}, \quad U_0/M_{\text{Pl}}^4 = -2.36 \times 10^{-7}, \\ S_{\text{end}}/v_S &= 1.09, \quad S_*/v_S = 2.30, \quad \Lambda_H/M_{\text{Pl}} = 2.48 \times 10^{-1}. \end{aligned} \quad (3.28)$$

## D. Numerical study

### 1. Independent parameters

Using the method described in the previous sections, we now scan the parameter space spanned by  $\lambda_S, y, \beta, \gamma$ . As we will show below, the inflational parameters,  $n_s, r$  and  $\beta^2 A_s$ , depend approximately only on  $\lambda_S, y, \bar{\gamma}$ , where

$$\bar{\gamma} = \frac{\gamma}{\beta^2}, \quad (3.29)$$

which makes a comprehensive analysis easier. To see this, we recall how the final single-field potential  $V_{\text{inf}}(S) = V(S, \sigma_v, \varphi_v)$  (3.18) is obtained, where  $V(S, \sigma, \varphi)$  and  $\varphi_v$  are given in Eqs. (3.10) and (3.12), respectively, while  $\sigma_v$  should be calculated from  $\partial\tilde{V}(S, \sigma)/\partial\sigma\big|_{\sigma=\sigma_v} = 0$ , where  $\tilde{V}(S, \sigma) = V(S, \sigma, \varphi_v)$  (3.13). As we see from Eq. (3.4), only  $U(S, \sigma)$  depends on  $\sigma$ , where the  $\sigma$  dependence enters due to the NJL potential  $V_{\text{NJL}}(S, \sigma)$  (2.10). Therefore, we find

$$0 = \frac{\partial\tilde{V}}{\partial\sigma}\bigg|_{\sigma=\sigma_v} = \frac{B^2 M_{\text{Pl}}^8}{(16GU + B^2 M_{\text{Pl}}^4)^2} \frac{\partial U}{\partial\sigma}\bigg|_{\sigma=\sigma_v} \rightarrow 0 = \frac{\partial V_{\text{NJL}}}{\partial\sigma}\bigg|_{\sigma=\sigma_v}. \quad (3.30)$$

Note that  $V_{\text{NJL}}(S, \sigma)$  does not depend on  $\lambda_S, \beta$  and  $\gamma$ , which implies that  $\sigma_v$  does not depend on  $\lambda_S, \beta$  and  $\gamma$ .

As a next step, we redefine  $B(S), G(S)$  and  $\tilde{V}(S, \sigma)$  as follows:

$$\bar{B}(S) = \frac{B(S)M_{\text{Pl}}^2}{\beta} = S^2 \left( 1 + \frac{3\lambda_S}{16\pi^2} \ln[3\lambda_S S^2/v_S^2] \right), \quad (3.31)$$

$$\bar{G}(S) = \frac{G(S)}{\beta^2} = \bar{\gamma} - \frac{1 + \ln[3\lambda_S S^2/v_S^2]}{64\pi^2}, \quad (3.32)$$

$$\bar{V}(S, \sigma) = \frac{\beta^2}{M_{\text{Pl}}^4} \tilde{V}(S, \sigma) = \frac{\beta^2 U(S, \sigma)}{16G(S)U(S, \sigma) + B(S)^2 M_{\text{Pl}}^4} = \frac{U(S, \sigma)}{16\bar{G}(S)U(S, \sigma) + \bar{B}(S)^2}. \quad (3.33)$$

Thus, the  $\beta$  dependence disappears in the above functions, if one uses  $\bar{\gamma}$  (3.29) as an independent parameter. Recalling  $V_{\text{inf}}(S) = \tilde{V}(S, \sigma_v)$ , we find that  $V'_{\text{inf}}/V_{\text{inf}}$  and  $V''_{\text{inf}}/V_{\text{inf}}$ , which enter in  $\varepsilon$  (3.20),  $\eta$  (3.21) and  $N_e$  (3.22), do not depend on  $\beta$ . Therefore, since we can use

$$\bar{V}_{\text{inf}}(S) = \bar{V}(S, \sigma_v) = \frac{\beta^2}{M_{\text{Pl}}^4} V_{\text{inf}}(S, \sigma) \quad (3.34)$$

to calculate these slow role parameters, the  $\beta$  independence of  $\bar{V}'_{\text{inf}}/\bar{V}_{\text{inf}}$  and  $\bar{V}''_{\text{inf}}/\bar{V}_{\text{inf}}$  appearing in the slow role parameters becomes trivial.

So far the above discussion on the  $\beta$  independence is exact. There is in fact an origin of the  $\beta$  dependence in the slow role parameters: The function  $F(S)$ , that is defined in Eq. (3.16) and is used to define the canonically normalized field  $\hat{S}$  in Eq. (3.19), enters in these parameters. To see it more explicitly, we square the both sides of Eq. (3.19) and obtain

$$\frac{F(S)^2}{M_{\text{Pl}}^2} = \beta^{-1} \times \frac{1 + Z_\sigma^{-1} \sigma_v'^2}{(1 + 4A) \bar{B}} + \frac{3}{2} \frac{((1 + 4A) \bar{B}' + 4A' \bar{B})^2}{(1 + 4A)^2 \bar{B}^2}, \quad (3.35)$$

where  $A(S, \sigma)$  is independent of  $\beta$ , because

$$A(S, \sigma) = \frac{4G(S)U(S, \sigma)}{B(S)^2 M_{\text{Pl}}^4} = \frac{4\bar{G}U(S, \sigma)}{\bar{B}(S)^2}. \quad (3.36)$$



Since the wave function renormalization  $Z_\sigma^{-1}$  ( $\simeq 0.3$ ) and  $\sigma_v$  are also independent of  $\beta$ , the  $\beta$  dependence of  $F(S)$  can be simply factorized as we see in the first term of Eq. (3.35). Note that in our parameter space the ratio of the first term without  $\beta$  to the second term is of order  $10^{-1}$  and  $\beta \gtrsim 10^2$ . Consequently, the  $\beta$  dependence in  $F(S)$  becomes negligibly small. We therefore shall ignore the first term in Eq. (3.35) in performing a parameter scan, so that the independent parameters are  $\lambda_S, y$  and  $\bar{\gamma}$ .

As announced, we impose the constraint (3.24) on  $A_s$ , which explicitly depends on  $\beta$ . Fortunately, this dependence is so simple, that it can be absorbed as

$$\bar{A}_s = \beta^2 A_s = \frac{\beta^2 V_{\text{inf}}(S_*)}{24\pi^2 \varepsilon_* M_{\text{Pl}}^4} = \frac{\bar{V}_{\text{inf}}(S_*)}{24\pi^2 \varepsilon_*}, \quad (3.37)$$

where  $\bar{V}_{\text{inf}}$  is defined in Eq. (3.34). Obviously,  $\bar{A}_s$  does not depend on  $\beta$ . Thus, we calculate first  $n_s, r, N_e$  and  $\bar{A}_s$  for a given set of  $\lambda_S, y, \bar{\gamma}$ , and using the constraint on  $A_s$  (3.24) we determine the value of  $\beta$  from  $\beta = 10^5(\bar{A}_s/e^{3.044})^{1/2}$  and then  $\gamma$  from  $\gamma = \bar{\gamma}\beta^2$ .

## 2. Result

The results are shown in Figs. 4, 5, and 6 for  $\lambda_S = 1.20 \times 10^{-2}$ ,  $1.20 \times 10^{-6}$ , and 1.20, respectively. In the left panels we show the values for  $\beta$  and  $\gamma$ , while in the right panels the corresponding values of  $n_s$  and  $r$  together with  $N_e$  are presented.

If we vary  $\bar{\gamma} = \gamma/\beta^2$  with  $\ln(10^{10}A_s) = 3.044$  fixed, we have a line in the  $\gamma - \beta$  plane as we can see in the left panels. For a given set of  $\lambda_S, y$  and  $N_e$ , the prediction becomes a line in the  $n_s - r$  plane, because we vary  $\bar{\gamma}$ . Therefore, there is a one-to-one correspondence between the lines in the left panels and right panels. The  $y$  dependence of  $n_s$  and  $r$  is indeed small, but  $\Lambda_H/M_{\text{Pl}}$  is quite different as we can see from Eqs. (3.25) and (3.28). By comparing Fig. 4 with Fig. 6, we can also see that  $n_s$  becomes larger if  $\lambda_S$  becomes larger. The solid (dashed) blue lines in the right panels indicates the two-(one-)  $\sigma$  constraint by Planck [34, 35]. We see that the model predictions are in good agreement with the observed data.

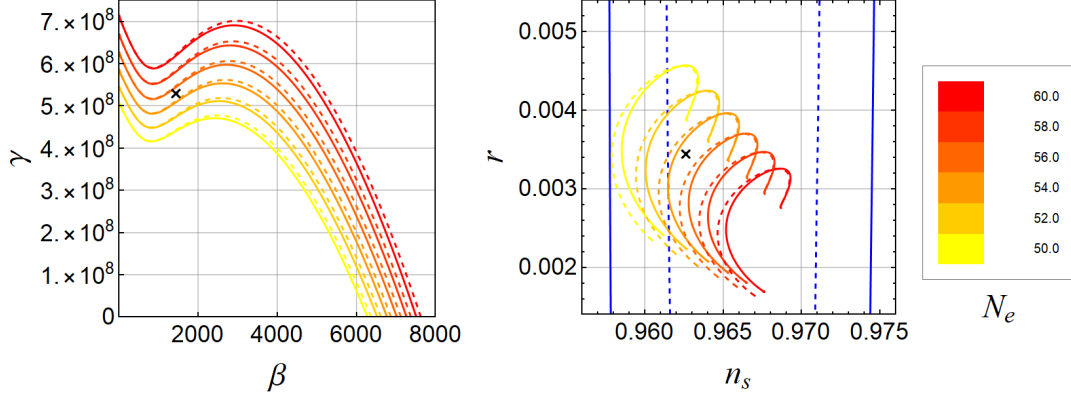


FIG. 4. The prediction on the inflationary parameters for  $\lambda_S = 1.20 \times 10^{-2}$  and  $y = 4.00 \times 10^{-3}$  (solid line) and  $4.00 \times 10^{-4}$  (dashed line), while the color represents  $N_e$ . The benchmark point (3.26) is marked by a cross. Left:  $\beta$  and  $\gamma$  that satisfy Eq. (3.24). Right: The prediction in the  $n_s - r$  plane, where the solid (dashed) blue lines are two (one)  $\sigma$  constraint by Planck [34, 35].

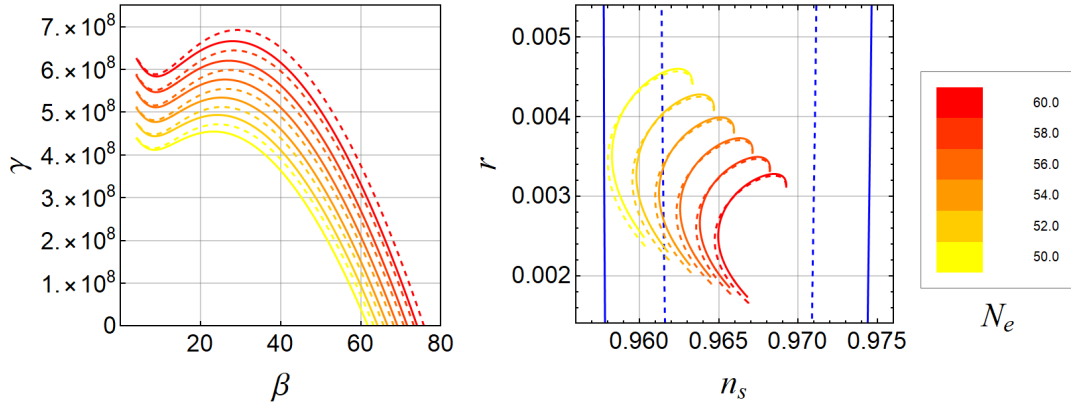


FIG. 5. The same as for Fig. 4 for  $\lambda_S = 1.20 \times 10^{-6}$ .

## IV. DARK MATTER

### A. Mass spectrum and dark matter candidate

Once the VEVs of  $\sigma$  and  $S$  are obtained, the scalar masses can be calculated by integrating out the hidden fermions. These CP even scalars mix with each other, and the corresponding two point functions at the one-loop level  $\Gamma_{AB}(A, B = S, \sigma)$  in the  $SU(3)_V$  flavor symmetry

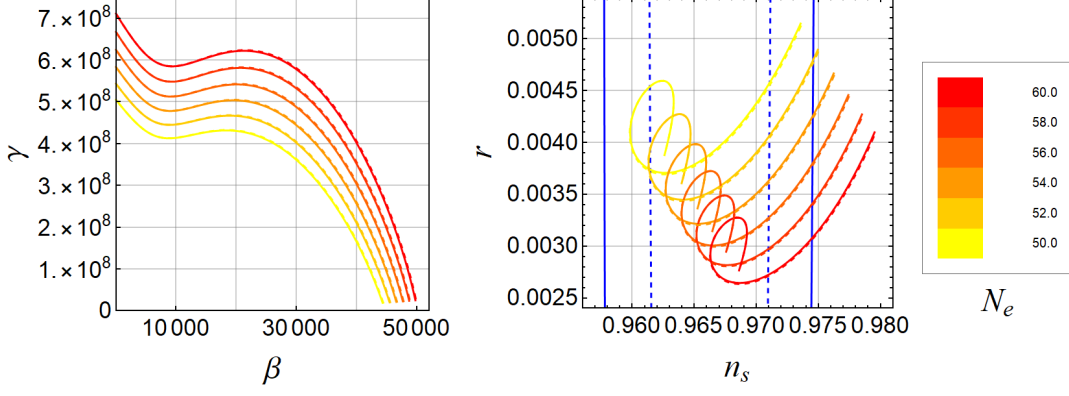


FIG. 6. The same as for Fig. 4 for  $\lambda_S = 1.20$ .

limit are given by [49, 51, 52].

$$\begin{aligned}
\Gamma_{SS}(p^2) &= p^2 - 3\lambda_S \langle S \rangle^2 - y^2 3n_c I_{\varphi^2}(p^2, M, \Lambda_H), \\
\Gamma_{S\sigma}(p^2) &= -y \left( 1 - \frac{G_D \langle \sigma \rangle}{4G^2} \right) 3n_c I_{\varphi^2}(p^2, M, \Lambda_H), \\
\Gamma_{\sigma\sigma}(p^2) &= -\frac{3}{4G} + \frac{3G_D \langle \sigma \rangle}{8G^3} - \left( 1 - \frac{G_D \langle \sigma \rangle}{4G^2} \right)^2 3n_c I_{\varphi^2}(p^2, M, \Lambda_H) + \frac{G_D}{G^2} 3n_c I_V(M, \Lambda_H),
\end{aligned} \tag{4.1}$$

where we have neglected the Higgs portal coupling, and the loop functions are defined as

$$\begin{aligned}
I_{\varphi^2}(p^2, M, \Lambda) &= \int_{\Lambda} \frac{d^4 k}{i(2\pi)^4} \frac{\text{Tr}(\not{k} + \not{p} + M)(\not{k} + M)}{((k+p)^2 - M^2)(k^2 - M^2)}, \\
I_V(M, \Lambda) &= \int_{\Lambda} \frac{d^4 k}{i(2\pi)^4} \frac{M}{(k^2 - M^2)} = -\frac{1}{16\pi^2} M \left[ \Lambda^2 - M^2 \ln \left( 1 + \frac{\Lambda^2}{M^2} \right) \right].
\end{aligned} \tag{4.2}$$

The mixed fields  $(S, \sigma)$  and the diagonalized fields  $(S_1, S_2)$  corresponding to the mass eigenstates are related by

$$\begin{pmatrix} S \\ \sigma \end{pmatrix} = \begin{pmatrix} \xi_S^{(1)} & \xi_S^{(2)} \\ \xi_\sigma^{(1)} & \xi_\sigma^{(2)} \end{pmatrix} \begin{pmatrix} S_1 \\ S_2 \end{pmatrix}, \tag{4.3}$$

where we denote the mass of  $S_i$  by  $m_i$ . The mixing parameters  $\xi_{S,\sigma}^{(i)}$  and  $m_i$  can be obtained by solving

$$\sum_{B=S,\sigma} \Gamma_{AB}(m_i^2) \xi_B^{(i)} = 0. \tag{4.4}$$

For the benchmark point given in Eq. (3.14), we find <sup>9</sup>:

$$m_1/\Lambda_H \simeq 0.044, \quad m_2/\Lambda_H \simeq 0.41, \\ \xi_S^{(1)} \simeq 1.00, \quad \xi_\sigma^{(1)} \simeq 0.01, \quad \xi_S^{(2)} \simeq -0.006, \quad \xi_\sigma^{(2)} \simeq 1.00. \quad (4.5)$$

Therefore, the mixing is very small, and we find that  $m_1$  can be well approximated by  $\tilde{m}_S = \sqrt{3\lambda_S}v_S$ . We have calculated  $m_1/\Lambda_H$  and  $m_2/\Lambda_H$  as a function of  $y$  and  $\lambda_S$  for an area in the parameter space which is relevant for our purpose. This is plotted in Fig.7, where the size of  $m_i/\Lambda_H$  is shown with a color graduation. (The data points satisfy  $m_\phi > m_1$ , where  $m_\phi$  is calculated from Eq. (4.6).) We find that the mixing between  $S$  and  $\sigma$  in the

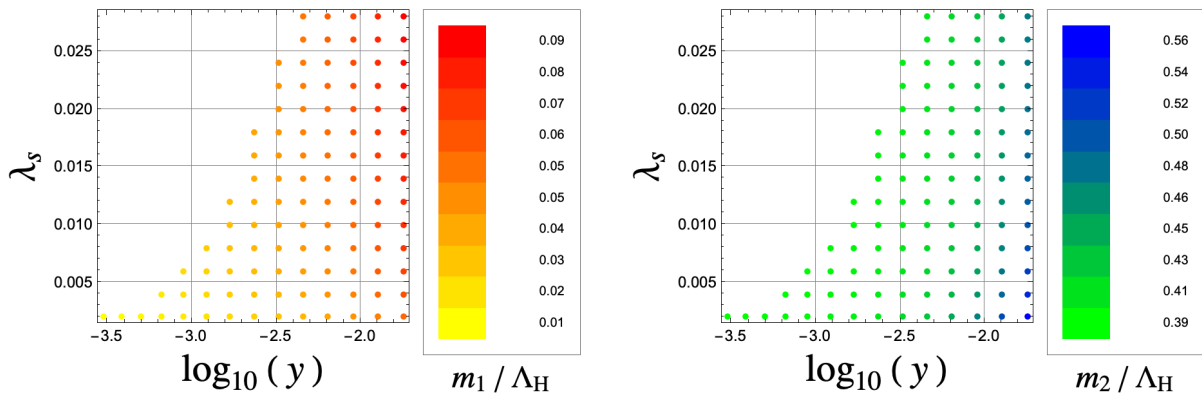


FIG. 7. The parameter space in the  $y - \lambda_S$  plane that we consider. The data points are so chosen that  $m_\phi > m_1$  is satisfied, where  $m_\phi$  is calculated from Eq. (4.6). The size of  $m_1/\Lambda_H$  and  $m_2/\Lambda_H$  is shown with a color graduation. In the most of the parameter space the mixing between  $S$  and  $\sigma$  is negligibly small, and  $m_1 \simeq \tilde{m}_S = \sqrt{3\lambda_3}v_S$  is satisfied.

parameter space is very small as it is the case for the example shown in Eq. (4.5). We also find that in the most of the area of the parameter space  $m_1 \ll m_2$  and  $m_1 \simeq \sqrt{3\lambda_S}v_S$  are satisfied. Therefore,  $\sigma$  will not play any role for our discussion below, and we use the approximate formula  $m_1 \simeq \tilde{m}_S$  in the following discussions.

Due to the vector-like flavor symmetry (i.e.  $SU(3)_V$  or its subgroup), the dark meson, the CP-odd scalar  $\phi_a$  in Eq. (2.7), is a good DM candidate. The two point function at the

<sup>9</sup> The mixing matrix in Eq. (4.3) is not an orthogonal matrix. This means that after diagonalization one has to perform an appropriate wave function renormalization to define canonically normalized fields. Since the mixing is very small and we are mostly interested in  $S$  being inflaton, we ignore this procedure here.

one-loop level for  $\phi_a$  is written as [49, 51, 52]

$$\Gamma_\phi(p^2) = -\frac{1}{2G} + \frac{G_D \langle \sigma \rangle}{8G^3} + \left(1 - \frac{G_D \langle \sigma \rangle}{8G^2}\right)^2 2n_c I_{\phi^2}(p^2, M, \Lambda_H) + \frac{G_D}{G^2} n_c I_V(M, \Lambda_H), \quad (4.6)$$

where the loop function  $I_{\phi^2}(p^2, M, \Lambda)$  is given by

$$I_{\phi^2}(p^2, M, \Lambda) = \int_\Lambda \frac{d^4 k}{i(2\pi)^4} \frac{\text{Tr}(\not{k} - \not{p} + M)\gamma_5(\not{k} + M)\gamma_5}{((k-p)^2 - M^2)(k^2 - M^2)}, \quad (4.7)$$

and  $m_\phi$  is defined by  $\Gamma_\phi(m_\phi^2) = 0$ . For the benchmark point we find  $m_\phi/\Lambda_H \simeq 0.06 > \tilde{m}_S/\Lambda_H$ . This implies that, if  $S$  is inflaton, it cannot decay into the dark meson<sup>10</sup>. As we see from Fig. (7),  $m_\phi > \tilde{m}_S$  is satisfied in the most of the parameter space, especially for large  $y (\gtrsim 0.003)$ . We therefore break  $SU(3)_V$  down to  $SU(2)_V \times U(1)$  and assume a hierarchy in the Yukawa couplings [52]:

$$\mathbf{y} = \text{diag.}(y_1, y_1, y_3) \text{ with } y_1 = y_2 < y_3, \quad (4.8)$$

where  $\mathbf{y}$  is the Yukawa matrix in the hidden sector described by the Lagrangian (2.1). Under this assumption, the dark mesons fall into three categories,  $\tilde{\pi} = \{\tilde{\pi}^\pm, \tilde{\pi}^0\}$ ,  $\tilde{K} = \{\tilde{K}^\pm, \tilde{K}^0, \tilde{\bar{K}}^0\}$  and  $\tilde{\eta}$ . Here the dark mesons are named like the real-world mesons:

$$\begin{aligned} \tilde{\pi}^\pm &\equiv (\phi_1 \mp i\phi_2)/\sqrt{2}, \quad \tilde{\pi}^0 \equiv \phi_3, \\ \tilde{K}^\pm &\equiv (\phi_4 \mp i\phi_5)/\sqrt{2}, \quad \tilde{K}^0(\tilde{\bar{K}}^0) \equiv (\phi_6 + (-)i\phi_7)/\sqrt{2}, \quad \tilde{\eta}^8 \equiv \phi_8, \end{aligned} \quad (4.9)$$

where  $\tilde{\eta}^8$  will mix with  $\tilde{\eta}^0 = \phi_0$  to form the mass eigenstates  $\tilde{\eta}$  and  $\tilde{\eta}'$ . The states in the same category have the same mass,  $m_{\tilde{\pi}^0} = m_{\tilde{\pi}^\pm} (\equiv m_{\tilde{\pi}})$  and  $m_{\tilde{K}^\pm} = m_{\tilde{K}^0} = m_{\tilde{\bar{K}}^0} (\equiv m_{\tilde{K}})$ , with  $m_{\tilde{\pi}} < m_{\tilde{K}} < m_{\tilde{\eta}}$ . As we will see in the next section, the dark meson mass has to be several orders of magnitude smaller than  $\tilde{m}_S$ , such that we can obtain a realistic DM abundance. The dark meson mass decreases as the Yukawa coupling decreases. However, if we decrease by several orders of magnitude, the cutoff  $\Lambda_H$  increases accordingly and may exceed  $M_{\text{Pl}}$  by various orders of magnitude, which we want to avoid. A nice way out exists if there is a parameter space in which  $m_{\tilde{\pi}} \ll \tilde{m}_S < m_{\tilde{K}} < m_{\tilde{\eta}}$  is realized, as we will argue in the next section when discussing DM relic abundance.

<sup>10</sup> The dark meson  $\phi_a$  can also be produced by the annihilation of  $N$ . However, as shown in the next subsection, its cross section is very small due to the small  $y_M$ . Therefore we consider the DM production from inflaton decay.

If  $SU(3)_V$  is broken to the  $SU(2)_V \times U(1)$ , Eq. (4.6) is no longer applicable to obtain the dark meson mass. Fortunately, there exists a good approximation [72]

$$m_{\tilde{\pi}}^2/m_{\phi}^2 \simeq m_u/m_q \simeq y_1/y, \quad (4.10)$$

where  $m_u$  is the current quark mass in the  $SU(2)_V \times U(1)$  case, and  $m_q$ ,  $m_{\phi}$  and  $y$  are the current quark mass, the dark meson mass and the Yukawa coupling, respectively, in the  $SU(3)_V$  limit. In Fig. 8 we show  $m_{\tilde{\pi}}/m_{\tilde{\pi}}^{\text{exact}}$  for  $3 \times 10^{-14} < y_1 < 3 \times 10^{-6}$  (while  $\tilde{m}_S < m_{\tilde{K}}$  is satisfied), where  $m_{\tilde{\pi}}^{\text{exact}}$  is the dark pion mass calculated by using the formula of Ref. [52] for the  $SU(2)_V \times U(1)$  case. As we see from Fig. 8 the difference between  $m_{\tilde{\pi}}$  and  $m_{\tilde{\pi}}^{\text{exact}}$  is

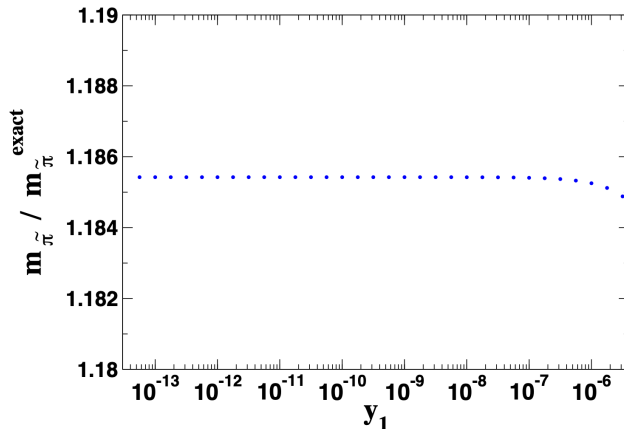


FIG. 8. The ratio  $m_{\tilde{\pi}}/m_{\tilde{\pi}}^{\text{exact}}$  against  $y_1$ , where  $m_{\tilde{\pi}}$  is calculated by using Eq. (4.10), and  $m_{\tilde{\pi}}^{\text{exact}}$  is calculated by using the formula of Ref. [52] for the  $SU(2)_V \times U(1)$  case.

less than 20% for a wide range of  $y_1$ , and we shall use this approximation.

The message of this section is that there exists a sufficiently large parameter space, in which  $m_{\tilde{\pi}} \ll \tilde{m}_S < m_{\tilde{K}} < m_{\tilde{\eta}}$  can be realized.

## B. Dark matter relic abundance

Dark matter can be produced during or after the reheating phase, see e.g. [73–75]. In the following discussions we assume that the Yukawa couplings  $y_1$  and  $y_3$  are so chosen that the mass hierarchy  $2m_{\tilde{\pi}} < \tilde{m}_S < m_{\tilde{K}} < m_{\tilde{\eta}}$  is satisfied. Under this assumption the inflaton  $S$

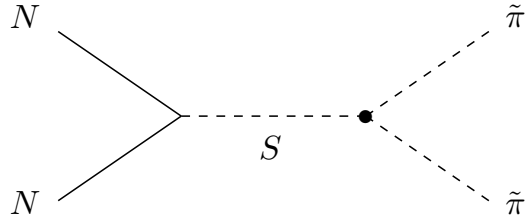


FIG. 9. The annihilation process  $N N \leftrightarrow \tilde{\pi} \tilde{\pi}$ , where the  $N - N - S$  coupling is  $y_M = m_N/v_S$  and the  $\tilde{\pi} - \tilde{\pi} - S$  effective coupling (indicated by a bullet) is denoted  $G_{\tilde{\pi}\tilde{\pi}S}$  in the text, which can be calculated from the diagrams shown in Fig. 10 [52].

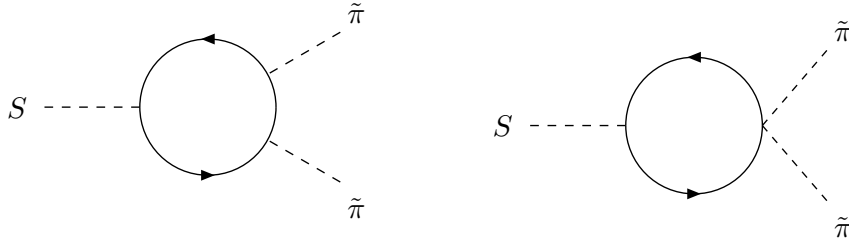


FIG. 10. One-loop diagrams contributing to the effective coupling  $G_{\tilde{\pi}\tilde{\pi}S}$ , which has been calculated in Ref. [52].

can decay only into a pair of  $\tilde{\pi}$  - which is our DM - but not into the other mesons, and therefore they are not produced during the reheating stage and later [74].  $\tilde{\pi}$  can also be produced by the annihilation process  $N N \leftrightarrow \tilde{\pi} \tilde{\pi}$ . The corresponding  $S$  channel diagram is shown in Fig. 9. As we see from this diagram, the annihilation cross section is proportional to  $y_M^2 G_{\tilde{\pi}\tilde{\pi}S}^2$ , where  $G_{\tilde{\pi}\tilde{\pi}S}^2$  is the effective  $S - \tilde{\pi} - \tilde{\pi}$  coupling. Since  $y_M^2 \sim m_N^2/v_S^2 \sim 10^{-18}$ , the  $\tilde{\pi}$  production through the annihilation process is negligibly small compared with that through the decay which is proportional only to  $G_{\tilde{\pi}\tilde{\pi}S}^2$ . Therefore, we ignore this annihilation process and take into account only the decay of  $S$  into  $\tilde{\pi}$ , with the decay width

$$\gamma_{\tilde{\pi}} = \frac{3 G_{\tilde{\pi}\tilde{\pi}S}^2}{16\pi\tilde{m}_S} \sqrt{1 - \frac{4m_{\tilde{\pi}}^2}{\tilde{m}_S^2}}, \quad (4.11)$$

where the effective coupling is calculated in Ref. [52] from the diagram shown in Fig. (10) and is found to be  $G_{\tilde{\pi}\tilde{\pi}S}/\Lambda_H \simeq -0.012 y_1$  for  $y_1 \lesssim 5 \times 10^{-4}$ .

In this way we arrive at a system, which consists of only the inflaton  $S$  and the  $\tilde{\pi}$ . The evolution of the number densities,  $n_S$  and  $n_{\tilde{\pi}}$ , can be described by the coupled Boltzmann equations [73]

$$\frac{dn_S}{dt} = -3Hn_S - \Gamma_S n_S, \quad (4.12)$$

$$\frac{dn_{\tilde{\pi}}}{dt} = -3Hn_{\tilde{\pi}} + \gamma_{\tilde{\pi}} n_S, \quad (4.13)$$

where  $\Gamma_S$  is the total decay width of  $S$ . Eq. (4.12) can be simply solved [76]:

$$n_S(a) = \frac{\rho_{\text{end}}}{\tilde{m}_S} \left[ \frac{a_{\text{end}}}{a} \right]^3 e^{-\Gamma_S(t-t_{\text{end}})}, \quad (4.14)$$

where  $a$  is the scale factor at  $t > t_{\text{end}}$ ,  $a_{\text{end}}$  is  $a$  at the end of inflation  $t_{\text{end}}$  and  $\rho_{\text{end}} = \rho_S(a_{\text{end}}) = \tilde{m}_S n_S(a_{\text{end}})$  is the inflaton energy density at  $t_{\text{end}}$ . Then we insert the solution (4.14) into Eq. (4.13) to find

$$n_{\tilde{\pi}}(a) = B_{\tilde{\pi}} \frac{\rho_{\text{end}}}{\tilde{m}_S} \left[ \frac{a_{\text{end}}}{a} \right]^3 (1 - e^{-\Gamma_S(t-t_{\text{end}})}) \quad \text{with } B_{\tilde{\pi}} = \frac{\gamma_{\tilde{\pi}}}{\Gamma_S}, \quad (4.15)$$

from which we obtain the DM relic abundance

$$\Omega_{\tilde{\pi}} h^2 = m_{\tilde{\pi}} B_{\tilde{\pi}} \frac{\rho_{\text{end}}}{\tilde{m}_S} \left[ \frac{a_{\text{end}}}{a_0} \right]^3 \frac{1}{3M_{\text{Pl}}^2 (H_0/h)^2}, \quad (4.16)$$

where  $a_0 = 1$  and  $H_0 = h 2.1332 \times 10^{-42}$  GeV with  $h \simeq 0.674$  [34] stand for the present value of the scale factor and the Hubble parameter, respectively. To proceed, we write the ratio  $a_{\text{end}}/a_0$  as

$$\frac{a_{\text{end}}}{a_0} = R_{\text{rad}} F_{\text{LA}} \left( \frac{\sqrt{3} H_0}{\rho_{\text{end}}^{1/4}} \right), \quad (4.17)$$

where

$$R_{\text{rad}} = \left( \frac{a_{\text{end}}}{a_{\text{RH}}} \right) \left( \frac{\rho_{\text{end}}^{1/4}}{\rho_{\text{RH}}^{1/4}} \right) = \left( \frac{\rho_{\text{RH}}}{\rho_{\text{end}}} \right)^{\frac{1-3\bar{w}}{12(1+\bar{w})}} \quad (4.18)$$

with  $\bar{w}$  being the average equation of state [77], and

$$F_{\text{LA}} = \frac{a_{\text{RH}} \rho_{\text{RH}}^{1/4}}{\sqrt{3} a_0 H_0} = \exp \left( 66.89 - \frac{1}{12} \ln g_{\text{RH}} \right), \quad (4.19)$$

with  $g_{\text{RH}}$  being the relativistic degrees of freedom at the end of reheating [35, 78]. The average equation of state  $\bar{w}$  is zero in the present case, because  $V_{\text{inf}}(S)$  in Eq. (3.18) behaves



as  $V_{\text{inf}}(\hat{S}) \sim \hat{S}^2$  near the potential minimum, where  $\hat{S}$  is the canonically normalized field and defined in Eq. (3.19). Consequently, the  $\rho_{\text{end}}$  dependence in  $\Omega_{\tilde{\pi}} h^2$  cancels. Further, introducing the reheating temperature  $T_{\text{RH}}$  as

$$\rho_{\text{RH}} = \frac{\pi^2}{30} g_{\text{RH}} T_{\text{RH}}^4, \quad (4.20)$$

we find [74].

$$\begin{aligned} \Omega_{\tilde{\pi}} h^2 &= \sqrt{3} \exp(3 \times 66.89) \frac{B_{\tilde{\pi}} H_0 h^2}{M_{\text{Pl}}^2} \left( \frac{\pi^2}{30} \right)^{1/4} \left( \frac{m_{\tilde{\pi}}}{\tilde{m}_S} \right) T_{\text{RH}} \\ &\simeq 2.04 \times 10^8 B_{\tilde{\pi}} \left( \frac{m_{\tilde{\pi}}}{\tilde{m}_S} \right) \frac{T_{\text{RH}}}{1 \text{ GeV}}. \end{aligned} \quad (4.21)$$

The branching ratio  $B_{\tilde{\pi}} = \gamma_{\tilde{\pi}}/\Gamma_S$  can be obtained from  $\gamma_{\tilde{\pi}}$  given in Eq. (4.11) together with the assumption that  $1/\Gamma_S$  is the time scale at the end of the reheating phase [73, 76], which means  $1/H(a_{\text{RH}}) = (3 M_{\text{Pl}}^2/\rho_{\text{RH}})^{1/2}$ .

### C. Reheating temperature and DM relic abundance

As we see from Eq. (4.21), we need to know the reheating temperature  $T_{\text{RH}}$  to obtain an actual value of the DM relic abundance  $\Omega_{\tilde{\pi}} h^2$ . Fortunately, it is possible [77, 79] to constrain the reheating phase and hence  $T_{\text{RH}}$  for a given inflation model without specifying reheating mechanism. We will follow this idea to find consistent values for  $T_{\text{RH}}$  for our model.

The basic unknown quantities during the reheating phase are the expansion rate  $a_{\text{end}}/a_{\text{RH}}$  and the energy density  $\rho_{\text{RH}}$  at the end of reheating. These uncertainties can be taken into account in  $R_{\text{rad}}$  [77], which has been already introduced in Eq. (4.18). We then consider the ratio  $a_{\text{end}}/a_*$ , where  $a_* = k_*/H_*$  is the scale factor at the time of CMB horizon exit,  $k_*$  is the pivot scale set by the Planck mission [34, 35], and  $H_*$  is the Hubble parameter at  $a = a_*$ :

$$a_{\text{end}}/a_* = R_{\text{rad}} F_{\text{LA}} \left( \sqrt{3} H_*/\rho_{\text{end}}^{1/4} \right) (a_0 H_0/k_*). \quad (4.22)$$

( $F_{\text{LA}}$  is given in Eq. (4.19)). Using Eq. (4.22) we find that the number of e-folds  $N_e$  can be written as [77, 80]

$$\begin{aligned} N_e &= \ln \left( \frac{a_{\text{end}}}{a_*} \right) = 66.89 - \frac{1}{12} \ln g_{\text{RH}} + \frac{1}{12} \ln \left( \frac{\rho_{\text{RH}}}{\rho_{\text{end}}} \right) + \frac{1}{4} \ln \left( \frac{V_{\text{inf}*}^2}{M_{\text{Pl}}^4 \rho_{\text{end}}} \right) - \ln \left( \frac{k_*}{a_0 H_0} \right) \\ &= 66.80 - \ln \left( \frac{k_*}{a_0 H_0} \right) + \frac{1}{4} \ln \left( \frac{V_{\text{inf}*}^2}{M_{\text{Pl}}^4 \rho_{\text{end}}} \right) - \frac{1}{12} \ln \left( \frac{V_{\text{end}}(3 - \varepsilon_*)}{(3 - \varepsilon_{\text{end}}) M_{\text{Pl}}^4} \right) + \frac{1}{3} \ln \left( \frac{T_{\text{RH}}}{M_{\text{Pl}}} \right), \end{aligned} \quad (4.23)$$

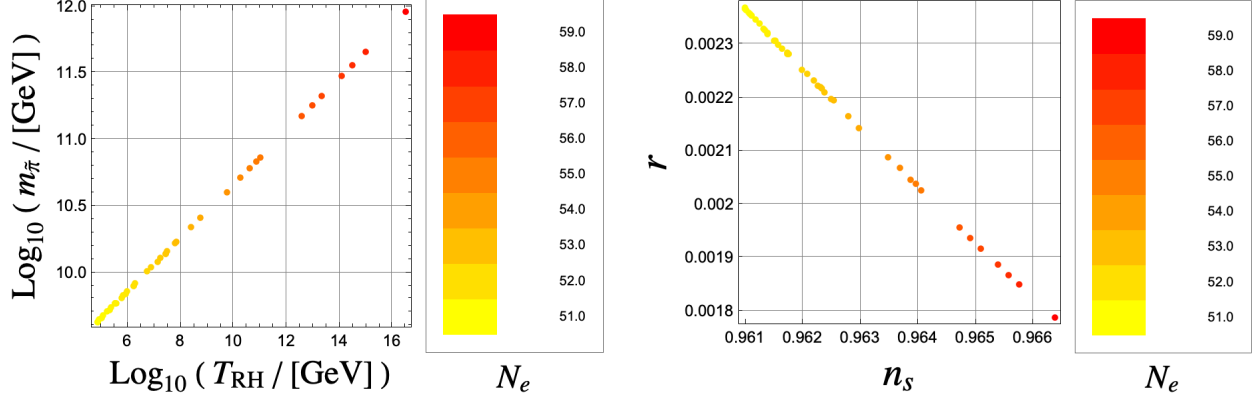


FIG. 11. Left: Dark matter mass  $m_{\tilde{\pi}}$  against the reheating temperature  $T_{\text{RH}}$ . The colored points satisfy  $\Omega_{\tilde{\pi}} h^2 = 0.1198 \pm 0.0024 (2\sigma)$ , where the color represents the e-foldings  $N_e$ . We have varied  $y_1$  and  $\gamma$  for fixed  $y_3$ ,  $\beta$  and  $\lambda_S$  at  $4.00 \times 10^{-3}$ ,  $6.31 \times 10^3$  and  $1.2 \times 10^{-2}$ , respectively, such that the constraint on  $A_s$  given in Eq. (3.24) is satisfied. Note that the lower bound on  $T_{\text{RH}}$  for a viable thermal leptogenesis with  $m_N \gtrsim 2 \times 10^7$  GeV is about  $10^9$  GeV [81]. Right: The same points as in the left panel are displayed in the  $n_s - r$  plane.

where we have used

$$\sqrt{3}H_* = \frac{V_{\text{inf}*}^{1/2}}{M_{\text{Pl}}} \quad \text{and} \quad \rho_{\text{end}} = \frac{V_{\text{end}}(3 - \varepsilon_*)}{(3 - \varepsilon_{\text{end}})}, \quad (4.24)$$

and  $V_{\text{end}} = V_{\text{inf}}(S_{\text{end}})$ ,  $V_{\text{inf}*} = V_{\text{inf}}(S_*)$ ,  $\varepsilon_{\text{end}} = \varepsilon(S_{\text{end}})$ , and  $\varepsilon_* = \varepsilon(S_*)$ . Note that the  $g_{\text{RH}}$  dependence in Eq. (4.23) disappears.

For the benchmark point (3.14) (see also (3.25) and (3.26)) with  $y_3 = 4.00 \times 10^{-3}$  and  $y_1 = 4.47 \times 10^{-13}$ , we find

$$\begin{aligned} \Lambda_H &\simeq 1.30 \times 10^{17} \text{ GeV}, \quad m_{\tilde{\pi}} \simeq 8.31 \times 10^{10} \text{ GeV}, \quad \tilde{m}_S \simeq 5.67 \times 10^{15} \text{ GeV}, \\ G_{\tilde{\pi}\tilde{\pi}S} &\simeq -2.35 y_1 \times 10^{15} \text{ GeV} \simeq -1.05 \times 10^3 \text{ GeV}, \\ T_{\text{RH}} &\simeq 2.07 \times 10^{11} \text{ GeV}, \quad B_{\tilde{\pi}} \simeq 1.90 \times 10^{-16}, \end{aligned} \quad (4.25)$$

which gives  $\Omega_{\tilde{\pi}} h^2 \simeq 0.119$ . In Figs. 11 and 12 (left) we show the points in the  $T_{\text{RH}} - m_{\tilde{\pi}}$  plane, for which  $\Omega_{\tilde{\pi}} h^2 = 0.1198 \pm 0.0024 (2\sigma)$  is obtained. Note that  $m_{\tilde{\pi}}$  (4.10) and  $\gamma_{\tilde{\pi}}$  (4.11) appearing in  $\Omega_{\tilde{\pi}} h^2$  (4.21) strongly depend on  $y_1$ , so that they are closely correlated. We have varied  $y_1$  and  $\gamma$  ( $\lambda_S$ ) for Fig. 11 (12) for fixed  $y_3$ ,  $\beta$  and  $\lambda_S$  ( $\gamma$ ), such that the constraint (3.24) is satisfied. In the right panel we show the corresponding values of  $n_s$  and  $r$ .

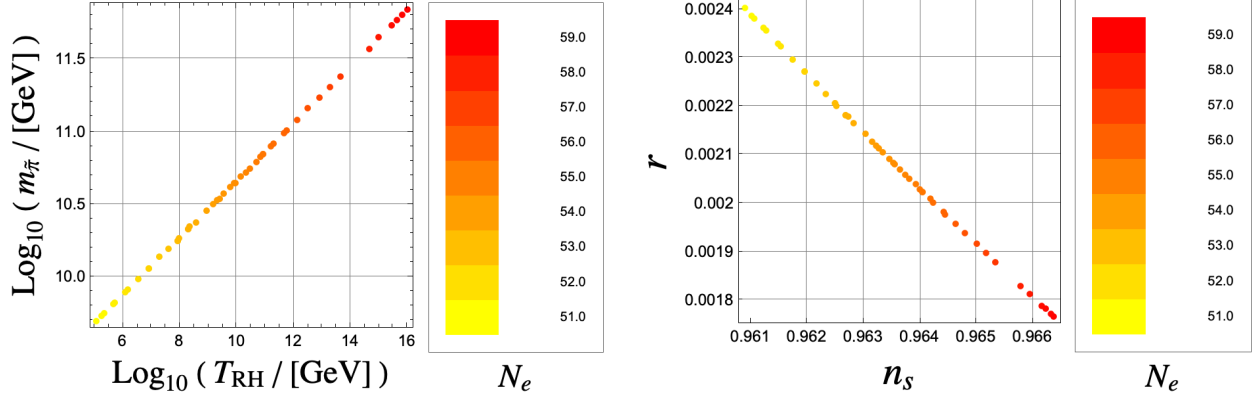


FIG. 12. The same as Fig.11 with  $y_3 = 4.00 \times 10^{-3}$ ,  $\beta = 6.31 \times 10^3$ ,  $\gamma = 1.26 \times 10^8$ , while  $\lambda_S$  and  $y_1$  are varied.

## V. CONCLUSION

We have followed John Wheeler’s requirement [82] that the fundamental equations should not contain any dimensionful parameter. Accordingly, we have started with a theory, which contains no dimensionful parameter at the classical level. Since there exists energy scales in the real world, they have to be generated. We have two known mechanisms of “scalegenesis” at hand; the Coleman-Weinberg mechanism and the dynamical symmetry breaking by strong dynamics in nonabelian gauge theories. The former mechanism is based on improved perturbation theory, while the later one uses nonperturbative effect in nonabelian gauge theories, e.g., chiral symmetry breaking in QCD, which produces about 99 % of the proton mass.

In this paper we have assumed that the origin of the dimensionful parameters, i.e. the Planck mass and the electroweak scale including the right-handed neutrino mass, is chiral symmetry breaking in a QCD-like theory, which couples with the visible sectors only via a real scalar  $S$ , the mediator. It is not only a mediator, but also inflaton, which makes a Higgs-inflation-like scenario possible. In fact the prediction of the CMB observables, the scalar spectral index  $n_s$  and the tensor-to-scalar ratio  $r$ , is similar to that of the Higgs-inflation [9] (or  $R^2$  inflation [29–31]). It will be our next task to find out differences. Since there are two more independent parameters compared with the Higgs inflation and three-field system is approximated by a single-field system, such differences should exist in particular in the primordial non-Gaussianity in the cosmological density perturbations which manifests itself

in the CMB anisotropy [83]. We will come to address these problems elsewhere.

The chiral symmetry breaking in the hidden sector produces (quasi) NG bosons in the same way as in QCD. Due to the Yukawa coupling of  $S$  with the hidden fermions, which explicitly breaks the chiral symmetry, the (quasi) NG bosons are massive. In contrast to the case of QCD they are stable because of the unbroken vector-like flavor symmetry and therefore can be DM candidates. We have however realized that the full  $SU(3)_V$  flavor group has to be broken to obtain a realistic DM relic abundance. The reason is that the (quasi) NG boson mass decreases as the Yukawa coupling  $y$  decreases, while the energy scale of the hidden sector  $\Lambda_H$  increases (because the scales of the visible sectors are fixed). The only viable scenario for a realistic DM in our model is the decay from inflaton  $S$ . For that to work the Yukawa coupling should be very small to sufficiently suppress the decay width ( $\propto y^2$ ), which would imply that  $\Lambda_H$  would be several orders of magnitude larger than  $M_{\text{Pl}}$ . If on the other hand  $SU(3)_V$  is explicitly broken to  $SU(2)_V \times U(1)$ , we have two Yukawa couplings  $y_1 = y_2$  and  $y_3$ . For large  $y_3 \simeq 10^{-3}$  and small  $y_1 \simeq 10^{-14 \sim -13}$ , which gives  $\Lambda_H/M_{\text{Pl}} \simeq 10^{-1}$  and  $m_{\text{DM}} (\propto \sqrt{y_1/y_3}) \simeq 10^{9 \sim 12}$  GeV, the DM relic abundance can become comparable with the observed value. Unfortunately, it will be impossible to directly detect our DM, because it is too heavy, and the interaction with the visible sector is suppressed by  $y_1$  and hence negligibly small.

## ACKNOWLEDGMENTS

J. K. would like to thank J. Kuntz, M. Lindner, J. Rezaeck, P. Saake and A. Trautner for useful and interesting discussions. The work of M. A. is supported in part by the Japan Society for the Promotion of Sciences Grant-in-Aid for Scientific Research (Grant No. 17K05412 and No. 20H00160). J. K. is partially supported by the Grant-in-Aid for Scientific Research (C) from the Japan Society for Promotion of Science (Grant No.19K03844). J. Y. is supported by the China Scholarship Council and the Japanese Government (Monbukagakusho-MEXT) scholarship.

---

[1] S. R. Coleman and E. J. Weinberg, *Radiative Corrections as the Origin of Spontaneous Symmetry Breaking*, *Phys. Rev. D* **7** (1973) 1888–1910.

- [2] Y. Nambu, *Axial vector current conservation in weak interactions*, *Phys. Rev. Lett.* **4** (1960) 380–382.
- [3] Y. Nambu and G. Jona-Lasinio, *Dynamical Model of Elementary Particles Based on an Analogy with Superconductivity I*, *Phys. Rev.* **122** (1961) 345–358.
- [4] Y. Nambu and G. Jona-Lasinio, *Dynamical Model of Elementary Particles Based on an Analogy with Superconductivity II*, *Phys. Rev.* **124** (1961) 246–254. [,141(1961)].
- [5] C. Brans and R. H. Dicke, *Mach’s principle and a relativistic theory of gravitation*, *Phys. Rev.* **124** (1961) 925–935.
- [6] H. Terazawa, Y. Chikashige, K. Akama, and T. Matsuki, *Simple Relation Between the Fine Structure and Gravitational Constants*, *Phys. Rev. D* **15** (1977) 1181.
- [7] K. Akama, Y. Chikashige, T. Matsuki, and H. Terazawa, *Gravity and Electromagnetism as Collective Phenomena: A Derivation of Einstein’s General Relativity*, *Prog. Theor. Phys.* **60** (1978) 868.
- [8] H. Terazawa, *Cosmological Origin of Mass Scales*, *Phys. Lett. B* **101** (1981) 43–47.
- [9] F. Bezrukov and M. Shaposhnikov, *The standard model higgs boson as the inflaton*, *Physics Letters B* **659** (Jan, 2008) 703–706, [[0710.3755](#)].
- [10] M. Rinaldi and L. Vanzo, *Inflation and reheating in theories with spontaneous scale invariance symmetry breaking*, *Physical Review D* **94** (Jul, 2016) [[1512.07186](#)].
- [11] G. Tambalo and M. Rinaldi, *Inflation and reheating in scale-invariant scalar-tensor gravity*, *General Relativity and Gravitation* **49** (Mar, 2017) [[1610.06478](#)].
- [12] P. G. Ferreira, C. T. Hill, and G. G. Ross, *Scale-independent inflation and hierarchy generation*, *Physics Letters B* **763** (Dec, 2016) 174–178, [[1603.05983](#)].
- [13] P. G. Ferreira, C. T. Hill, and G. G. Ross, *No fifth force in a scale invariant universe*, *Physical Review D* **95** (Mar, 2017) [[1612.03157](#)].
- [14] P. G. Ferreira, C. T. Hill, J. Noller, and G. G. Ross, *Scale-independent  $R^2$  inflation*, *Physical Review D* **100** (Dec, 2019) [[1906.03415](#)].
- [15] J. Kubo, M. Lindner, K. Schmitz, and M. Yamada, *Planck mass and inflation as consequences of dynamically broken scale invariance*, *Phys. Rev. D* **100** (2019), no. 1 015037, [[1811.05950](#)].
- [16] J. Kubo, J. Kuntz, M. Lindner, J. Rezacek, P. Saake, and A. Trautner, *Unified emergence of energy scales and cosmic inflation*, *JHEP* **08** (2021) 016, [[2012.09706](#)].

- [17] A. H. Guth, *The Inflationary Universe: A Possible Solution to the Horizon and Flatness Problems*, *Phys. Rev.* **D23** (1981) 347–356.
- [18] A. D. Linde, *A New Inflationary Universe Scenario: A Possible Solution of the Horizon, Flatness, Homogeneity, Isotropy and Primordial Monopole Problems*, *Phys. Lett.* **108B** (1982) 389–393.
- [19] A. D. Linde, *Coleman-Weinberg Theory and a New Inflationary Universe Scenario*, *Phys. Lett.* **114B** (1982) 431–435.
- [20] A. Albrecht and P. J. Steinhardt, *Cosmology for Grand Unified Theories with Radiatively Induced Symmetry Breaking*, *Phys. Rev. Lett.* **48** (1982) 1220–1223.
- [21] A. D. Linde, *Inflationary Cosmology*, *Lect. Notes Phys.* **738** (2008) 1–54, [[0705.0164](#)].
- [22] A. Salvio and A. Strumia, *Agravity*, *JHEP* **06** (2014) 080, [[1403.4226](#)].
- [23] K. Kannike, G. Hütsi, L. Pizza, A. Racioppi, M. Raidal, A. Salvio, and A. Strumia, *Dynamically Induced Planck Scale and Inflation*, *JHEP* **05** (2015) 065, [[1502.01334](#)].
- [24] A. Karam, T. Pappas, and K. Tamvakis, *Nonminimal Coleman–Weinberg Inflation with an  $R^2$  term*, *JCAP* **02** (2019) 006, [[1810.12884](#)].
- [25] D. M. Ghilencea, *Weyl  $R^2$  inflation with an emergent Planck scale*, *JHEP* **10** (2019) 209, [[1906.11572](#)].
- [26] D. M. Ghilencea and H. M. Lee, *Weyl gauge symmetry and its spontaneous breaking in the standard model and inflation*, *Phys. Rev. D* **99** (2019), no. 11 115007, [[1809.09174](#)].
- [27] A. Farzinnia and S. Kouwn, *Classically scale invariant inflation, supermassive WIMPs, and adimensional gravity*, *Phys. Rev. D* **93** (2016), no. 6 063528, [[1512.05890](#)].
- [28] I. D. Gialamas, A. Karam, T. D. Pappas, and V. C. Spanos, *Scale-invariant quadratic gravity and inflation in the Palatini formalism*, *Phys. Rev. D* **104** (2021), no. 2 023521, [[2104.04550](#)].
- [29] A. A. Starobinsky, *A New Type of Isotropic Cosmological Models Without Singularity*, *Phys. Lett.* **B91** (1980) 99–102.
- [30] V. F. Mukhanov and G. V. Chibisov, *Quantum fluctuations and a nonsingular universe*, *Soviet Journal of Experimental and Theoretical Physics Letters* **33** (May, 1981) 532.
- [31] A. A. Starobinsky, *The Perturbation Spectrum Evolving from a Nonsingular Initially De-Sitter Cosmology and the Microwave Background Anisotropy*, *Sov. Astron. Lett.* **9** (1983) 302.

- [32] J. D. Barrow and S. Cotsakis, *Inflation and the Conformal Structure of Higher Order Gravity Theories*, *Phys. Lett. B* **214** (1988) 515–518.
- [33] K.-i. Maeda, *Towards the Einstein-Hilbert Action via Conformal Transformation*, *Phys. Rev. D* **39** (1989) 3159.
- [34] **Planck Collaboration**, Aghanim:2018eyx, *Planck 2018 results. VI. Cosmological parameters*, *Astron. Astrophys.* **641** (2020) A6, [[1807.06209](#)].
- [35] **Planck Collaboration**, Y. Akrami *et al.*, *Planck 2018 results. X. Constraints on inflation*, [[1807.06211](#)].
- [36] I. Brivio and M. Trott, *Radiatively Generating the Higgs Potential and Electroweak Scale via the Seesaw Mechanism*, *Phys. Rev. Lett.* **119** (2017), no. 14 141801, [[1703.10924](#)].
- [37] F. Vissani, *Do experiments suggest a hierarchy problem?*, *Phys. Rev. D* **57** (1998) 7027–7030, [[hep-ph/9709409](#)].
- [38] J. Casas, V. Di Clemente, A. Ibarra, and M. Quiros, *Massive neutrinos and the Higgs mass window*, *Phys. Rev. D* **62** (2000) 053005, [[hep-ph/9904295](#)].
- [39] J. D. Clarke, R. Foot, and R. R. Volkas, *Electroweak naturalness in the three-flavor type I seesaw model and implications for leptogenesis*, *Phys. Rev. D* **91** (2015), no. 7 073009, [[1502.01352](#)].
- [40] G. Bambhaniya, P. Bhupal Dev, S. Goswami, S. Khan, and W. Rodejohann, *Naturalness, Vacuum Stability and Leptogenesis in the Minimal Seesaw Model*, *Phys. Rev. D* **95** (2017), no. 9 095016, [[1611.03827](#)].
- [41] K. A. Meissner and H. Nicolai, *Conformal Symmetry and the Standard Model*, *Phys. Lett. B* **648** (2007) 312–317, [[hep-th/0612165](#)].
- [42] V. Brdar, Y. Emonds, A. J. Helmboldt, and M. Lindner, *Conformal Realization of the Neutrino Option*, *Phys. Rev. D* **99** (2019), no. 5 055014, [[1807.11490](#)].
- [43] P. Minkowski,  *$\mu \rightarrow e\gamma$  at a rate of one out of 109 muon decays?*, *Physics Letters B* **67** (1977), no. 4 421.
- [44] T. Yanagida, *Horizontal Symmetry and Masses of Neutrinos*, *Conf. Proc.* **C7902131** (1979) 95.
- [45] M. Gell-Mann, P. Ramond, and R. Slansky, *Complex Spinors and Unified Theories*, *Conf. Proc.* **C790927** (1979) 315, [[1306.4669](#)].

- [46] R. N. Mohapatra and G. Senjanović, *Neutrino mass and spontaneous parity nonconservation*, *Phys. Rev. Lett.* **44** (Apr, 1980) 912.
- [47] T. Hur and P. Ko, *Scale invariant extension of the standard model with strongly interacting hidden sector*, *Phys. Rev. Lett.* **106** (2011) 141802, [[1103.2571](#)].
- [48] M. Heikinheimo, A. Racioppi, M. Raidal, C. Spethmann, and K. Tuominen, *Physical Naturalness and Dynamical Breaking of Classical Scale Invariance*, *Mod. Phys. Lett.* **A29** (2014) 1450077, [[1304.7006](#)].
- [49] M. Holthausen, J. Kubo, K. S. Lim, and M. Lindner, *Electroweak and Conformal Symmetry Breaking by a Strongly Coupled Hidden Sector*, *JHEP* **12** (2013) 076, [[1310.4423](#)].
- [50] H. Hatanaka, D.-W. Jung, and P. Ko, *AdS/QCD approach to the scale-invariant extension of the standard model with a strongly interacting hidden sector*, *JHEP* **08** (2016) 094, [[1606.02969](#)].
- [51] J. Kubo, K. S. Lim, and M. Lindner, *Gamma-ray Line from Nambu-Goldstone Dark Matter in a Scale Invariant Extension of the Standard Model*, *JHEP* **09** (2014) 016, [[1405.1052](#)].
- [52] Y. Ametani, M. Aoki, H. Goto, and J. Kubo, *Nambu-Goldstone Dark Matter in a Scale Invariant Bright Hidden Sector*, *Phys. Rev.* **D91** (2015), no. 11 115007, [[1505.00128](#)].
- [53] I. Brivio and M. Trott, *Examining the neutrino option*, *JHEP* **02** (2019) 107, [[1809.03450](#)].
- [54] V. Brdar, A. J. Helmboldt, and J. Kubo, *Gravitational Waves from First-Order Phase Transitions: LIGO as a Window to Unexplored Seesaw Scales*, *JCAP* **02** (2019) 021, [[1810.12306](#)].
- [55] V. Brdar, A. J. Helmboldt, S. Iwamoto, and K. Schmitz, *Type-I Seesaw as the Common Origin of Neutrino Mass, Baryon Asymmetry, and the Electroweak Scale*, *Phys. Rev. D* **100** (2019) 075029, [[1905.12634](#)].
- [56] I. Brivio, K. Moffat, S. Pascoli, S. Petcov, and J. Turner, *Leptogenesis in the Neutrino Option*, *JHEP* **10** (2019) 059, [[1905.12642](#)]. [Erratum: *JHEP* 02, 148 (2020)].
- [57] M. Aoki, V. Brdar, and J. Kubo, *Heavy dark matter, neutrino masses, and Higgs naturalness from a strongly interacting hidden sector*, *Phys. Rev. D* **102** (2020), no. 3 035026, [[2007.04367](#)].
- [58] I. Brivio, J. Talbert, and M. Trott, *No-go limitations on UV completions of the Neutrino Option*, *Phys. Rev. D* **103** (2021), no. 1 015012, [[2010.15428](#)].



- [59] T. Kunihiro and T. Hatsuda, *A Selfconsistent Mean Field Approach to the Dynamical Symmetry Breaking: The Effective Potential of the Nambu-Jona-Lasinio Model*, *Prog. Theor. Phys.* **71** (1984) 1332.
- [60] T. Hatsuda and T. Kunihiro, *QCD phenomenology based on a chiral effective Lagrangian*, *Phys. Rept.* **247** (1994) 221–367, [[hep-ph/9401310](#)].
- [61] T. Inagaki, T. Muta, and S. D. Odintsov, *Nambu-Jona-Lasinio model in curved space-time*, *Mod. Phys. Lett. A* **8** (1993) 2117–2124, [[hep-th/9306023](#)].
- [62] T. Inagaki, T. Muta, and S. D. Odintsov, *Dynamical symmetry breaking in curved space-time: Four fermion interactions*, *Prog. Theor. Phys. Suppl.* **127** (1997) 93, [[hep-th/9711084](#)].
- [63] M. Aoki, H. Goto, and J. Kubo, *Gravitational Waves from Hidden QCD Phase Transition*, *Phys. Rev. D* **96** (2017), no. 7 075045, [[1709.07572](#)].
- [64] A. J. Helmboldt, J. Kubo, and S. van der Woude, *Observational prospects for gravitational waves from hidden or dark chiral phase transitions*, *Phys. Rev. D* **100** (2019), no. 5 055025, [[1904.07891](#)].
- [65] M. Aoki and J. Kubo, *Gravitational waves from chiral phase transition in a conformally extended standard model*, *JCAP* **04** (2020) 001, [[1910.05025](#)].
- [66] T. Markkanen, S. Nurmi, A. Rajantie, and S. Stopyra, *The 1-loop effective potential for the Standard Model in curved spacetime*, *JHEP* **06** (2018) 040, [[1804.02020](#)].
- [67] S. Weinberg, *The Cosmological Constant Problem*, *Rev. Mod. Phys.* **61** (1989) 1–23.
- [68] K. S. Stelle, *Classical Gravity with Higher Derivatives*, *Gen. Rel. Grav.* **9** (1978) 353–371.
- [69] L. Alvarez-Gaume, A. Kehagias, C. Kounnas, D. Lüst, and A. Riotto, *Aspects of Quadratic Gravity*, *Fortsch. Phys.* **64** (2016), no. 2-3 176–189, [[1505.07657](#)].
- [70] A. Salvio, *Quadratic Gravity*, *Front. in Phys.* **6** (2018) 77, [[1804.09944](#)].
- [71] D. Wands, *Multiple field inflation*, *Lect. Notes Phys.* **738** (2008) 275–304, [[astro-ph/0702187](#)].
- [72] M. Gell-Mann, R. J. Oakes, and B. Renner, *Behavior of current divergences under  $su_3 \times su_3$* , *Phys. Rev.* **175** (Nov, 1968) 2195–2199.
- [73] D. J. Chung, E. W. Kolb, and A. Riotto, *Production of massive particles during reheating*, *Phys. Rev. D* **60** (1999) 063504, [[hep-ph/9809453](#)].

- [74] R. Allahverdi and M. Drees, *Production of massive stable particles in inflaton decay*, *Phys. Rev. Lett.* **89** (2002) 091302, [[hep-ph/0203118](#)].
- [75] M. A. Garcia, K. Kaneta, Y. Mambrini, and K. A. Olive, *Reheating and Post-inflationary Production of Dark Matter*, *Phys. Rev. D* **101** (2020), no. 12 123507, [[2004.08404](#)].
- [76] E. W. Kolb and M. S. Turner, *The Early Universe*, vol. 69. 1990.
- [77] J. Martin and C. Ringeval, *First CMB Constraints on the Inflationary Reheating Temperature*, *Phys. Rev. D* **82** (2010) 023511, [[1004.5525](#)].
- [78] K. D. Lozanov and M. A. Amin, *Self-resonance after inflation: oscillons, transients and radiation domination*, *Phys. Rev. D* **97** (2018), no. 2 023533, [[1710.06851](#)].
- [79] A. R. Liddle and S. M. Leach, *How long before the end of inflation were observable perturbations produced?*, *Phys. Rev. D* **68** (2003) 103503, [[astro-ph/0305263](#)].
- [80] J. Martin, C. Ringeval, and V. Vennin, *Encyclopaedia Inflationaris*, *Phys. Dark Univ.* **5-6** (2014) 75–235, [[1303.3787](#)].
- [81] G. Giudice, A. Notari, M. Raidal, A. Riotto, and A. Strumia, *Towards a complete theory of thermal leptogenesis in the SM and MSSM*, *Nucl. Phys. B* **685** (2004) 89–149, [[hep-ph/0310123](#)].
- [82] F. Wilczek, *Mass without mass. I: Most of matter*, *Phys. Today* **52N11** (1999) 11–13.
- [83] N. Bartolo, E. Komatsu, S. Matarrese, and A. Riotto, *Non-Gaussianity from inflation: Theory and observations*, *Phys. Rept.* **402** (2004) 103–266, [[astro-ph/0406398](#)].